Thesis for the Degree of Doctor of Philosophy

Optimal Powertrain Dimensioning and Potential Assessment of Hybrid Electric Vehicles

Nikolce Murgovski

Department of Signals and Systems
Chalmers University of Technology
Göteborg, Sweden 2012

Optimal Powertrain Dimensioning and Potential Assessment of Hybrid Electric Vehicles

Nikolce Murgovski

ISBN 978-91-7385-682-9

Doktorsavhandlingar vid Chalmers tekniska högskola
Ny serie nr 3363
ISSN 0346-718X

Department of Signals and Systems
Chalmers University of Technology
SE–412 96 Göteborg
Sweden

Telephone: +46 (0)31 772 1000

Typeset by the author using LaTeX.

Chalmers Reproservice
Göteborg, Sweden 2012

To my beloved
Jordanka.

Abstract

Hybrid electric vehicles (HEVs), compared to conventional vehicles, complement the traditional combustion engine with one, or several electric motors and an energy buffer, typically a battery and/or an ultracapacitor. This gives the vehicle an additional degree of freedom that allows for a more efficient operation, by e.g. recuperating braking energy, or operating the engine at higher efficiency.

In order to be cost effective, the HEV may need to include a downsized engine and a carefully selected energy buffer. The optimal size of the powertrain components depends on the powertrain configuration, ability to draw electric energy from the grid, charging infrastructure, drive patterns, varying fuel, electricity and energy buffer prices and on how well adapted is the buffer energy management to driving conditions.

This thesis provides two main contributions for optimal dimensioning of HEV powertrains while optimally controlling the energy use of the buffer on prescribed routes. The first contribution is described by a methodology and a tool for potential assessment of HEV powertrains. The tool minimizes the need for interaction from the user by automizing the processes of powertrain simplification and optimization. The HEV powertrain models are simplified by removing unnecessary dynamics in order to speed up computation time and allow Dynamic Programming to be used to optimize the energy management. The tool makes it possible to work with non-transparent models, e.g. models which are compiled, or hidden for intellectual property reasons.

The second contribution describes modeling steps to reformulate the powertrain dimensioning and control problem as a convex optimization problem. The method considers quadratic losses for the powertrain components and the resulting problem is a semidefinite convex program. The optimization is time efficient with computation time that does not increase exponentially with the number of states. This makes it possible to include more accurate models in the optimization, e.g. powertrain components with thermal properties.

Keywords: Hybrid electric vehicle, plug-in/slide-in HEV, powertrain sizing, power management, Dynamic Programming, convex optimization.

Acknowledgments

I would like to express my gratitude to my supervisor Prof. Jonas Sjöberg for the much needed guidance in the beginning and the persisting support throughout my studies. I would also like to thank Prof. Per-Olof Gutman and the coauthors of my papers: Prof. Bo Egardt, Docent Jonas Fredriksson, Docent Anders Grauers, Dr. Jonas Hellgren and MSc. Bengt Norén. My sincere gratitude to my colleagues and friends at the Signals and Systems department.

Studying for a PhD is like carrying a heavy load on a bumpy road. Dr. Lars Johannesson was the person clearing that road for me. Thank you Lars for the never ending discussions, valuable ideas, encouragement and friendship. I look forward to working together on the many interesting projects to come.

Good research requires fulfillment in not only professional, but also in personal life. Thereby, I would like to thank all my friends who brought joy in my life and endured the discussions about my "exciting" work. Thanks to my family who supported me throughout this journey. And finally, I cannot express my thanks enough to the person who stood by my side for nearly a decade. Jordanka, you have been the pillar of my life, and I hope I will always have you for the joy, patience, encouragement and love you give.

Nikolce Murgovski
Göteborg, 05 2012

List of publications

This thesis is based on the following appended papers:

Paper 1

N. Murgovski, J. Sjöberg, J. Fredriksson, A methodology and a tool for evaluating hybrid electric powertrain configurations, *Int. J. Electric and Hybrid Vehicles, vol. 3, no. 3, p. 219-245, 2011.*

Paper 2

N. Murgovski, L. Johannesson, J. Sjöberg, B. Egardt, Component sizing of a plug-in hybrid electric powertrain via convex optimization, *J. Mechatronics, vol. 22, no. 1, p. 106-120, 2012.*

Paper 3

N. Murgovski, L. Johannesson, J. Sjöberg, Convex modeling of energy buffers in power control applications, *Submitted to the IFAC Workshop on Engine and Powertrain Control, Simulation and Modeling (ECOSM), Rueil-Malmaison, France.*

Paper 4

N. Murgovski, L. Johannesson, A. Grauers, J. Sjöberg, Dimensioning and control of a thermally constrained double buffer plug-in HEV powertrain, *Submitted to the 51st IEEE Conference on Decision and Control, Maui, Hawaii.*

Paper 5

N. Murgovski, L. Johannesson, J. Sjöberg, Engine on/off control for dimensioning hybrid electric powertrains via convex op-

timization, *Submitted to the IEEE Transactions on Vehicular Technology*.

Other publications

In addition to the appended papers, the following papers authored or co-authored by N. Murgovski are related to the topic of the thesis:

M. Pourabdollah, N. Murgovski, A. Grauers, B. Egardt, Optimal sizing of a parallel PHEV powertrain, *Submitted to the IEEE Transactions on Vehicular Technology*.

N. Murgovski, L. Johannesson, J. Hellgren, B. Egardt, J. Sjöberg, Convex optimization of charging infrastructure design and component sizing of a plug-in series HEV powertrain, *IFAC World Congress, Milan, Italy, 2011*.

N. Murgovski, J. Sjöberg, J. Fredriksson, A tool for generating optimal control laws for hybrid electric powertrains, *IFAC Symposium on Advances in Automotive Control, Munich, Germany, 2010*.

N. Murgovski, J. Fredriksson, J. Sjöberg, B. Norén, Hybrid powertrain concept evaluation using optimization, *Electric Vehicle Symposium (EVS25), Shenzhen, China, 2010*.

N. Murgovski, J. Sjöberg, J. Fredriksson, Automatic simplification of hybrid powertrain models for use in optimization, *Symposium on Advanced Vehicle Control (AVEC10), Loughborough, UK, 2010*.

Contents

Part I

Introductory part

Chapter 1

Introduction

This chapter gives an overview of electric and hybrid electric vehicles, it introduces the powertrain dimensioning and control problem, and emphasizes the main contributions of this thesis.

1.1 A brief history of electrified vehicles

The first appearance of electric vehicles (EVs) dates back to the early 1830. These EVs were not commercial vehicles as they used non-rechargeable batteries. It will take an additional half a century before batteries are developed sufficiently to be used in commercial vehicles [1]. That period, from about 1895 to 1905, is also the EVs' golden age of dominance in the market when they outsold all other types of cars in USA [2, 3]. This is the period when pneumatic tires were being introduced, although some early commercial EVs still had wheels with wooden spokes and solid rubber tires (Figure 1.1). In about the same period, hybrid EVs (HEVs) were also introduced. In 1989 Ferdinand Porsche, an employee of the Austrian company Jacob Lohner & Co, developed a drive system based on fitting an electric motor to each front wheel, without using a transmission [4]. The powertrain was a series hybrid, with an engine-generator unit providing electricity to drive the wheel motors (Figure 1.2).

The reasons for the success of EVs were some features that are still advantageous over petroleum powered vehicles. EVs are silent, clean, free of vibrations, do not consume energy while being stopped, do not produce dirt and odor, and are easier to control as gear shifting may not be required. The disadvantages of the EVs are basically the disadvantages of the batteries, i.e. high initial cost or short range, reaction to heat and cold, long charging time, short calendar life, etc.

During the 20th century petroleum powered vehicles showed absolute

Figure 1.1: William Morrison Electric Wagon, 1892 [3].

Figure 1.2: The first HEV by Dr. Ferdinand Porsche [4].

dominance over the EVs. The reasons are easily understood when the specific energy of petroleum fuel is compared to that of batteries. For example, the specific energy of diesel, i.e. energy stored per kilogram, is about 12 600 Wh/kg, while the highest reported specific energy of Lithium-air batteries is about 360 Wh/kg [5, 6]. Moreover, the diesel is much cheaper with 0.15 €/kWh, compared to the optimistic price of about 180 €/kWh for energy optimized batteries projected by the United States Advanced Battery Consortium [7].

The electrification of vehicles has increased again in the 21st century motivated by the air pollution, global warming and rapid depletion of the Earth's petroleum resources. In order to develop efficient and cost effective powertrain technology, HEVs are being reintroduced as a short-term solution. HEVs have the potential to decrease fuel consumption and emissions, without a serious impact on vehicle's performance. Moreover, with a carefully dimensioned vehicle powertrain, e.g. downsized engine and relatively small battery, it is possible to make the cost of HEVs comparable with convectional vehicles in the same performance category.

1.2 HEV powertrain topologies

Similarly as any vehicle powertrain, HEVs' powertrains are required to 1) deliver sufficient power to meet the demands of vehicle performance; 2) support driving a given range without the need for refueling/recharging; 3) be energy efficient; 4) emit few environmental pollutants, etc. The difference with conventional vehicles is that HEVs have one or two additional degrees of freedom in achieving these requirements, because besides the internal combustion engine (ICE), HEVs utilize an energy buffer, typically a battery and/or an ultracapacitor, and one or more electric machines (EMs).

Depending on the division of power between the sources, HEVs can be commonly classified in three different topologies: series, parallel and series-parallel, depicted in Figure 1.3. The powertrain topologies mainly differ in the available degree of freedom in choosing the ICE operating point, but their capability to improve energy consumption can be generally described by:

- A possibility to recover braking energy by using the EMs as generators and storing the energy in the buffer;
- An ability to shut down the ICE during idling and low load demands;
- A possibility to run the ICE at more efficient load conditions while storing the excess energy in the buffer.

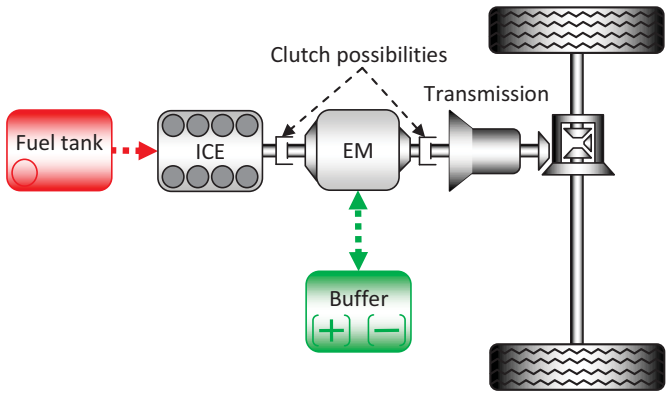

(a) Parallel HEV powertrain.

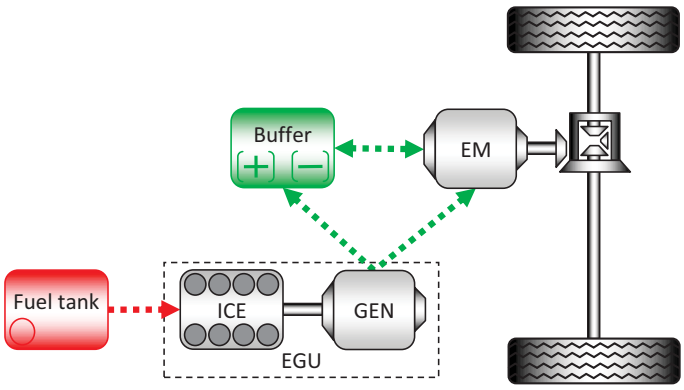

(b) Series HEV powertrain.

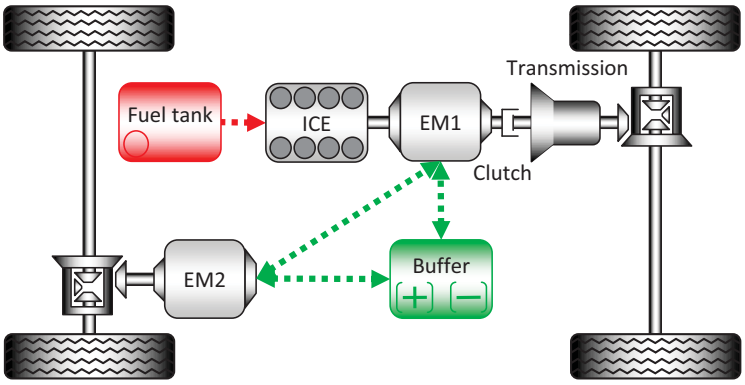

(c) Series-parallel (combined) HEV powertrain.

Figure 1.3: HEV powertrain topologies.

In the parallel topology, the ICE and EM are mounted on the same shaft which is mechanically linked to the wheels. The parallel HEVs considered in this thesis utilize the EM as in Figure 1.3(a), delivering power to the wheels via a transmission unit. In general, the EM can be also placed directly at the wheels and eventually, but not very common, at the rear axle. There is

also a possibility for including a clutch between the ICE and EM in addition to the clutch at the transmission. In Paper 1 an HEV is considered devoid of a clutch between the ICE and EM. This is typical for mild parallel HEVs where the EM is smaller and is not designed to drive the vehicle alone, but it is mainly used for starting (cranking) the ICE, or assisting with extra power. The disadvantage of this powertrain is that the EM will always need to rotate the ICE, even when the ICE is off, resulting in power losses. The parallel HEV considered in Paper 2 includes a clutch between the ICE and EM, giving a possibility to mechanically decouple the ICE, when the EM alone drives the vehicle.

The transmission used in this thesis consists of fixed gear steps, giving a limited freedom in choosing the ICE speed, depending on the number of gears. Other configurations with continuous variable transmission are also possible. With the gear ratio determined, the ICE torque can be freely chosen as the EM can give the remaining torque to satisfy the demanded power. Examples of commercial HEVs with a parallel powertrain are Honda Civic [8], Honda Insight [8], Volvo 7900 Hybrid Bus [9].

In the series topology, the ICE does not have a mechanical connection with the wheels, but it is coupled to a generator (GEN), as in Figure 1.3(b). Instead, the wheels are driven by an EM without the need for transmission. The ICE and GEN in this case are typically considered as one unit, i.e. engine-generator unit (EGU). The generator is in fact an EM that can be also used in motoring mode for starting up (cranking) the ICE before fuel is injected. The series powertrain offers a possibility to freely choose either the ICE speed, or the ICE torque, regardless of the vehicle speed. Generally, the torque-speed combination is chosen to optimize the EGU efficiency for a given demanded power. However, because of the losses in the two energy conversion stages, from petroleum to electric and from electric to mechanical, the series powertrain is generally disadvantageous with respect to fuel economy. This topology is competitive in driving scenarios with many start-stops and low power demands and therefore, it is mainly used in hybrid city buses. One example is the Orion city bus [10]. Another usage of this topology has been found in range extended EVs, where the range extender is an EGU with a significantly downsized and light weight ICE. These vehicles are hybrids, but are mainly intended to be used as electric vehicles during typical daily trips of less than 50 km. The responsibility of the range extender is to provide the additional millage on longer and not so common trips. An example of a range extended EV in a series topology is the Audi A1 e-tron [11], where the range extender is built upon a Wankel engine.

The series-parallel (combined) powertrain is a combination of the previ-

ous two. This powertrain allows the ICE to be decoupled from the wheels, as with the series powertrain, but it also allows for a mechanical link between the ICE and the wheels, as with the parallel powertrain. An example is the Toyota Prius powertrain [12] that uses planetary gear as a power split device, which offers possibility to freely choose both the engine speed and engine torque. The combined powertrain used in Paper 1 does not include a planetary gear, but it is constructed by extending a parallel powertrain with an EM mounted on the rear axle, as in Figure 1.3(c).

Other types of combined HEV powertrains which are not covered in this thesis are the two mode hybrid and the four quadrant transducer. The two mode hybrid [13] uses several planetary gears and clutches to achieve two modes of operation, a continuous variable transmission, and transmission with fixed gears. The use of the fixed gears in this topology reduces motor losses by decreasing the total amount of energy transmitted through the electrical path. This is particularly beneficial for vehicles with strong towing requirements and it is therefore mainly used in trucks and SUVs. Some examples are the Chevrolet's Tahoe, Silverado and Sierra hybrids [14].

The four quadrant transducer [15] is an electric machine consisting of two combined radial flux machines, one double rotor machine and one conventional machine (stator). This powertrain replaces the mechanical transmission with a magnetic path, thus providing smooth operation. As of March 2012, this topology has not yet been employed in commercial vehicles.

1.3 Plug-in HEV

Plug-in HEVs (PHEVs) are HEVs with an additional charging connector that allows them to draw electric energy from the grid. A distinction will be made here between personal passenger vehicles and PHEVs used in public transport. Personal PHEVs are designed to be charged with low power, e.g. a standard household electric power, and for longer periods. These PHEVs are mainly meant to be used as EVs and are typically charged overnight at home, or at parking locations at work, street, or commercial places.

The PHEVs considered in public transport are designed to charge with power as high as 250 kW and with charging times as short as 10 s. The PHEVs considered in this thesis, i.e. in Paper 2, 5 and 4, are city buses. Depending on the charging infrastructure, the PHEV bus may charge at the terminals, at charging stations placed on bus stops, or while driving along sections of the bus line. The charging solutions are generally classified in two groups: 1) conductive charging or wire coupling and 2) inductive charging or wireless coupling. The Autotram project [16], for example, considers a PHEV bus that charges from fast-charge docking stations while standing

still at stops along the bus line. The PHEV bus considered in [17] and [18] can charge with 250 kW for about 5 to 10 min while standing still at the terminals. In [19] the PHEV, a dual-mode trolley bus, can draw electricity from overhead wires, while driving along sections of an existing tram line. An example of using inductive chargers has been considered in the KAIST project [20], where the PHEV is charged while driving over underground cables that have been buried along sections of the bus line.

The cost effectiveness of these PHEVs depends strongly on the charging infrastructure, and in the optimal case, the PHEV powertrain should be designed together with the charging infrastructure. Optimization methods for dimensioning a PHEV bus have been presented in [21], where the considered charging infrastructure has a possibility for installing charging stations on different stops along the bus line.

1.4 Dimensioning an HEV powertrain

In order to be cost effective, the HEV is preferred to restore most of the braking energy, drive as long as possible on electric power and operate the ICE at more efficient load conditions. To achieve these goals, the HEV may need to include a downsized ICE and a carefully selected energy buffer that not only improves the system efficiency, but also does not significantly degrade vehicle performance, while keeping the price under reasonable limits. However, dimensioning the HEV powertrain is a difficult problem, because it depends not only on the powertrain configuration, but also on varying factors such as fuel, electricity and components prices. Ultracapacitors are an example of components with rapidly dropping prices. Maxwell Technologies[1], one of the leaders in the ultracapacitor industry, reported that the production cost for one of their mainstay products, a 3000 F cell, has been reduced by more than 10 times from the late 1990s to the beginning of 2009 [22].

It is even more challenging to size the powertrain of PHEV city buses, as buses may also have tight daily schedules with short charging intervals, or the charging infrastructure might be sparsely distributed. This puts hard constraints on the sizing of the energy buffer, i.e. determining power rating and energy capacity, and it may require using the buffer under high duty cycles, thus increasing its operating temperature and possible degrading its performance. To prevent overheating, the energy buffer should be managed properly, and/or the cooling system should be dimensioned at the same time when sizing the buffer.

[1] http://www.maxwell.com

Moreover, the energy efficiency of the powertrain also depends on how well adapted the energy management strategy is to the typical driving cycles of the vehicle [23]. The energy management strategy decides the operating point of the ICE and thereby when and at which rate the energy buffer is to be discharged. When optimizing the HEV based on a dynamic model of the powertrain, a badly designed energy management may lead to a non-optimal size of the powertrain components [24]. Hence, to overcome this problem, both the size of the powertrain components and the energy management need to be optimized simultaneously.

There are two main approaches to the problem of optimal sizing and control of HEVs. The first approach relies on heuristic algorithms [25, 26, 27, 28, 29, 30, 31, 32], while the second approach uses optimal control methods which give opportunity to evaluate various configurations on the basis of their optimal performance, when simulated along one or several drive cycles (e.g. speed vs. time profiles).

From the optimal control methods, Dynamic Programming (DP) [33] is the most commonly used [34, 35, 36, 37, 38, 39, 40, 41]. The main advantage with DP is the capability to use nonlinear, non-convex models of the components consisting of continuous and integer (mixed integer) optimization variables. Another important advantage is that the computation time increases linearly with the drive cycle length. However, DP has two important limitations when sizing powertrain components. The most serious limitation is that the computation time increases exponentially [33] with the number of state variables. As a consequence, the powertrain model is typically limited to only one or possibly two continuous state variables [34, 35, 36, 37, 38, 39, 40, 41]. More than three state variables would be highly impractical requiring a dedicated optimization code and a computer cluster. Moreover, since DP operates by recursively solving a smaller subproblem for each time step, the second limitation of DP is that it is not possible to directly include the component sizing into the optimization. Instead, DP must be run in several loops to obtain the optimal control over a grid of component sizes.

Another approach, proposed by [42], uses convex optimization for optimal control of HEVs. In this study the powertrain components of a series HEV powertrain are expressed with linear models and the optimization problem is a linear program. The problem of component sizing will then require running the algorithm in several loops for each fixed size of the components. The computation time is not a burden in this case, as convex problems are usually solved in seconds. However, linear models do not represent well the powertrain components which are better approximated with quadratic losses. Moreover, the linear model does not capture one

important limitation of the ICE, the low efficiency during idling.

1.5 Need for a novel systematic optimization

With the term optimization of an HEV powertrain this thesis distinguishes two problems, a problem of performance assessment of a powertrain with fixed components, and a problem of component sizing. In theory, the latter can be solved by iteratively solving the former over a grid of component sizes. Some tools that rely on this principle use detailed dynamic vehicle models (further explained in Section 2.2) and are typically not based on optimal vehicle performance. These tools are mainly used for modeling and simulation of HEVs with a limited support for evaluation of design parameters. Some examples are VEHLIB [43], AMESim, Dymola, JANUS [44], SIMPLEV [45], ADVISOR [46], [47], QSS-TB [48], HYSDEL [49], CAPSim [50], ADAMS/Car, CARSim and others [51, 52, 53, 54].

Other tools are based on optimal vehicle performance [55, 56, 48, 57, 58], where energy management is optimized by Dynamic Programming (DP). A limitation of these tools is that computation time increases exponentially with the number of state variables. Hence, to shorten the time, simplified quasi-static vehicle models are used (further explained in Section 2.4). However, even with simplified models, the problem of powertrain sizing will require iteratively running DP over a grid of component sizes, which again, will need long computation time.

This thesis investigates how to overcome several major difficulties in optimizing HEV powertrains based on optimal vehicle performance. In the general case this optimization problem is a non-convex, mixed integer problem, and therefore, DP is the algorithm traditionally used for optimization. Because DP uses a simplified powertrain model, this thesis investigates how to automize the process of model simplification and optimization with minimized need of interaction from the user. Moreover, to avoid the limitations of DP and thereby to allow simultaneous optimization of parameters deciding the component sizes (e.g. engine, battery, ultracapacitor, electric machine, etc.), this thesis investigates what approximations are needed to formulate the powertrain sizing and the corresponding optimal control problem as a convex optimization problem. The approximations need to be a fairly accurate representation of actual component data and should be at least as accurate as those already verified in literature. For example, the losses of the battery and the electric machine are typically considered quadratic, while the losses of the engine are affine on torque (but preferably quadratic), with speed dependent parameters [59, 60].

Finally, the optimization should overcome another limitation of DP, by

allowing more than two continuous states for describing the powertrain components. For example, the electrical components, such as the electric machine or the energy buffer, may be operated under high duty cycles and it is therefore reasonable to consider additional thermal states that will be optimally controlled in order to prevent preheating of the components.

1.6 Contribution of the thesis

This thesis contributes with methodologies for automatic and time efficient optimization of HEV powertrains. The main contributions are:

- A methodology for automatic simplification of HEV powertrain models with minimized need of interaction from the user. The simplified models are obtained in a form of static maps, which then allow Dynamic Programming to be used to optimize the energy management. The only requirement on the dynamic model is to provide access to some general variables and that it has a power split that can be fully controlled. This makes it possible to work with non-transparent models, e.g. models which are compiled, or hidden of intellectual property reasons. The methodology is developed and implemented in a tool that is useful for assessing the potential of an HEV powertrain. This contribution is detailed in Paper 1;

- A novel modeling approach that allows for a simultaneous powertrain dimensioning and HEV energy management by solving a semidefinite [61] convex problem. The method considers quadratic losses for the powertrain components and due to the short computation time it allows for optimal control of thermally constrained components. Convex modeling steps for dimensioning batteries with constant open circuit voltage have been described in Paper 2; dimensioning of ultracapacitors and batteries with linear voltage-state of charge dependency has been described in Paper 3; convex sizing of engine-generator unit and thermally constrained energy buffer is described in Paper 4; and a method for deciding integer control variables using convex optimization techniques is presented in Paper 5.

Chapter 2

Problem formulation and modeling details

This chapter formulates the powertrain sizing problem and gives a background on driving cycle and vehicle models. Most of the chapter repeats material from the articles, but explains modeling details in more depth and with more discussions.

2.1 Optimization problem

Without going into mathematical details, which will be described in the rest of this chapter, this section formulates the objective and briefly describes the constraints the optimization is subject to.

The studied sizing problem is formulated to simultaneously minimize an operational cost for driving the vehicle along a given cycle, and a component cost for the powertrain components that ought to be sized. The operational cost, considered in this thesis, includes cost for consumed fuel and electricity along the driven cycle, but in a general case, this cost may also include a cost for polluting the environment, or other costs penalizing specific operational modes of the powertrain (this is briefly discussed in Paper 1). The component cost is considered to include cost for the energy buffer, electric machine (EM), internal combustion engine (ICE), and engine-generator unit (EGU).

The optimization is subject to constraints that will be detailed in the rest of this chapter. Some constraints originate from the driven cycle (demanded speed and power as a function of time), others from the powertrain components and the power capabilities of the charging infrastructure. The constraints for components consist of physical limits, constraints imposed to prolong their calendar life, state equality constraints depicting power-

train dynamics, and desired initial and final state constraints. Finally, the optimization problem can be summarized as:

Minimize:

- Operational and component cost.

Subject to (at each point of time):

- Driving cycle constraints;
- Charging infrastructure constraints;
- Powertrain components constraints;
- States equality constraints;
- Initial and final state constraints.

2.2 Dynamic Vehicle Model

The dynamic vehicle model is a simplified representation of a real vehicle, which when simulated will produce output, e.g. fuel consumption, which accurately depicts the output of the real vehicle driven under same conditions. With the term dynamic model, this thesis will refer to the model of the vehicle, including a powertrain model, and a controller, including a driver model.

The vehicle simulation starts with the driver who attempts to follow a certain driving cycle represented by demanded speed $v_{dem}(t)$ and slope $\alpha_{dem}(t)$ as a function of time. In order to achieve the demanded velocity, the driver presses the gas pedal to accelerate the vehicle until its velocity is equal to the demanded velocity. This is called a forward simulation model. The model is a nonlinear hybrid-state system [62] that can be expressed as

$$\begin{aligned} \dot{x}_c(t) &= f_c(x(t), u_c(t)), \quad x_d^+(t) = f_d(x(t), u(t)) \\ y_c(t) &= g_c(x(t), u_c(t)), \quad y_d^+(t) = g_d(x(t), u(t)) \\ u(t) &= f_{ctrl}(x(t), y(t), v_{dem}(t), \alpha_{dem}(t)) \end{aligned} \tag{2.1}$$

with states $x(t)$, inputs $u(t)$ and outputs $y(t)$ given as

$$x(t) = \begin{bmatrix} x_c(t) \\ x_d(t) \end{bmatrix}, \quad y(t) = \begin{bmatrix} y_c(t) \\ y_d(t) \end{bmatrix}, \quad u(t) = \begin{bmatrix} u_c(t) \\ u_d(t) \end{bmatrix} \tag{2.2}$$

where $x_c(t)$, $u_c(t)$ and $y_c(t)$ are continuous states, inputs and outputs, respectively. The signals with index d take discrete values and change at

specific times. That is, e.g. $f_d(x(t), u(t))$ is constant (equal to $x_d(t)$) up to some time $\tilde{t}$ at which it jumps to a new value, i.e. $x_d^+(\tilde{t}) = f_d(x(\tilde{t}), u(\tilde{t}))$. After that f_d remains constant to the next jump in value. A PHEV model may have many continuous states, e.g. vehicle velocity, state of charge (SOC) of the energy buffer, and thermal states of the components. An example of a discrete state is the transmission gear, a continuous output is the fuel consumption, while a control signal is the power required by the energy buffer.

A dynamic vehicle model has been considered only in Paper 1, where disturbances to the continuous states have also been included. The rest of the papers use a simplified quasi-static vehicle model, described in details in Section 2.4.

2.3 Driving cycle and charging infrastructure model

The driving cycle model is described by demanded velocity $v_{dem}(t)$ and road slope $\alpha_{dem}(t)$ as functions of time. An example of a driving cycle, originating from a bus line in Gothenburg, is illustrated in Figure 2.1. The bus line also illustrates a charging infrastructure with three charging opportunities, where the bus may charge while standing still at both ends, and while driving at about the middle of the bus line. The charging could be either inductive from underground cables, or conductive from docking stations or overhead wires.

The PHEVs considered in this thesis are city buses which typically charge for short time intervals. Hence, it is reasonable to assume that the bus will charge mainly with high power at which constant average efficiency can be considered for both conductive and inductive chargers. Different chargers along the bus line may have different efficiencies and different power levels, which could be modeled by piecewise constant functions $\eta_c(t)$ and $P_{cmax}(t)$, respectively. These functions have non-zero values only in time intervals where charging opportunities exist (shaded in Figure 2.1).

The charging power $\boldsymbol{P_c}(t)$ the PHEV takes from the grid is considered an optimization (or decision) variable (optimization variables will be marked in bold), which is constrained by

$$\boldsymbol{P_c}(t) \in [0, P_{cmax}(t)]. \tag{2.3}$$

This gives an opportunity for the optimization to decide the amount of charging energy that will be taken from the grid. For example, instead of charging with maximum power, it may be found optimal to have smaller

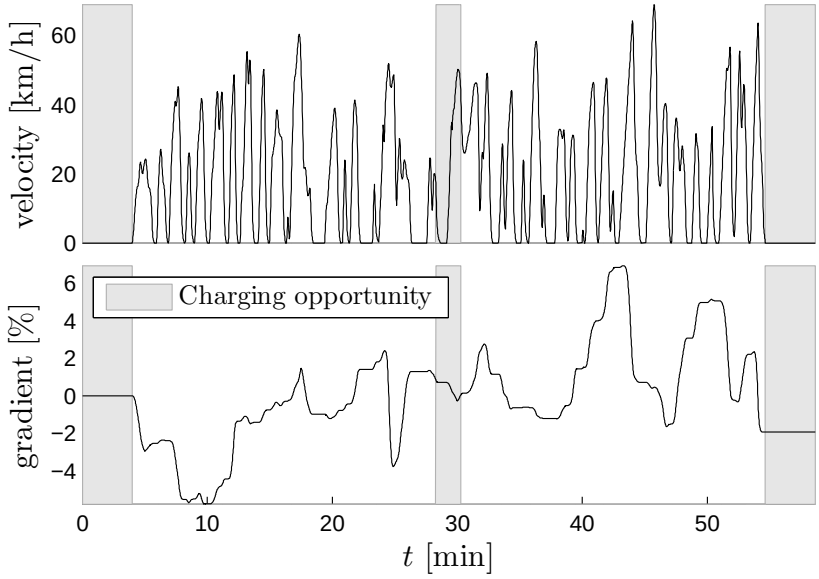

Figure 2.1: Bus line model described by demanded velocity and road gradient. The bus line has three charging opportunities, shaded in the figure. The bus can charge 4 min while standing still at each end, and 2 min at about the middle of the bus line, while driving along a tram line.

energy buffer that can be fully charged with less power. This outcome has been observed in Paper 4, indicating that charging stations could be downsized.

2.4 Quasi-static powertrain model

The quasi-static powertrain model is a backward simulation model of the HEV powertrain. From the demanded vehicle velocity and road gradient, the torque at the wheels is decided which will give the needed amount of fuel without necessitating a driver. In this process, the ICE and EM dynamics are omitted, the vehicle velocity is removed from the state vector, and only some slow dynamics are kept, e.g. the SOC of the energy buffer. Therefore, this model is referred to as quasi-static, and due to the low number of continuous states, it is favored because it exploits smaller simulation and optimization time. This level of details is often used when deciding control strategies, or comparing different vehicle concepts [36, 63, 64, 65].

In the rest of the thesis the HEV powertrain used in optimization is described by a quasi-static model. The vehicle is considered a point mass,

for which the longitudinal demanded force can be computed as

$$\begin{aligned} F_{dem}(\cdot) = &\left(\frac{J_v + r_{fg}^2 J_p(\cdot)}{R_w^2} + m(\cdot) \right) \dot{v}_{dem}(t) \\ &+ \frac{1}{2} \rho_{air} A_f c_d v_{dem}^2(t) + m(\cdot) g \left(c_r \cos \alpha_{dem}(t) + \sin \alpha_{dem}(t) \right). \end{aligned} \tag{2.4}$$

The symbol $\cdot$ denotes a compact notation for a function of decision variables, A_f is vehicle frontal area, c_d is aerodynamic drag coefficient, c_r is rolling resistance coefficient, ρ_{air} is air density, g is gravitational acceleration, R_w is wheel radius, r_{fg} is ratio of the final (differential) gear and J_v is rotational inertia of the wheels including the axles and the differential. The vehicle mass $m(\cdot)$ and the rotational inertia of the powertrain components $J_p(\cdot)$ may vary for different powertrain topologies and will be described in Section 2.4.1-2.4.3.

The losses of the power electronics are neglected, for simplicity, as they are typically much lower than the losses of the other powertrain components.

2.4.1 Parallel powertrain

The power balance equations for the parallel powertrain (illustrated in Figure 1.3(a)) can be described by

$$\begin{aligned} &F_{dem}(\cdot) v_{dem}(t) = \\ &\qquad (\boldsymbol{\tau_{EM}}(t) + \boldsymbol{\tau_{ICE}}(t)) \frac{v_{dem}(t)}{R_w} \left(\eta_\gamma(\boldsymbol{\gamma}(t)) \eta_{fg} \right)^{\operatorname{sign} F_{dem}(\cdot)} - \boldsymbol{P_{brk}}(t) \end{aligned} \tag{2.5}$$

$$\boldsymbol{\tau_{EM}}(t) \frac{v_{dem}(t)}{R_w} + B_{EM}(\cdot) = \boldsymbol{P_b}(t) + \boldsymbol{P_c}(t) \eta_c(t) - P_{aux} \tag{2.6}$$

where $\boldsymbol{P_{brk}}(t) \geq 0$ is braking power dissipated at the wheel brakes, $\boldsymbol{\tau_{EM}}(t)$ and $B_{EM}(\cdot)$ are torque and power loses of the EM, $\boldsymbol{\tau_{ICE}}(t)$ is torque of the ICE, $\boldsymbol{P_b}(t)$ is power of the energy buffer, $\eta_\gamma(\boldsymbol{\gamma}(t))$ is efficiency of transmission gear $\boldsymbol{\gamma}(t)$ and η_{fg} is efficiency of the final gear. For simplicity, the power used by auxiliary devices P_{aux} is assumed constant.

The rotational inertia of the powertrain components is described as

$$J_p(\cdot) = \left(J_{EM} + \boldsymbol{c}(t) J_{ICE} \right) r_\gamma^2(\boldsymbol{\gamma}(t)) + J_\gamma(\boldsymbol{\gamma}(t)) \tag{2.7}$$

where J_{EM}, J_{ICE} and $J_\gamma(\boldsymbol{\gamma}(t))$ are rotational inertias of the EM, ICE and transmission gear, $r_\gamma(\boldsymbol{\gamma}(t))$ is gear ratio and $\boldsymbol{c}(t)$ is a binary signal denoting the state of the clutch between the ICE and EM. The clutch near the transmission is considered as a transmission gear with zero ratio.

The vehicle mass is described as

$$m(\cdot) = m_v + m_{EM} + m_{ICE} + \boldsymbol{n_{bc}} m_{bc} \tag{2.8}$$

where m_v is the vehicle mass without the weight of the EM, ICE and energy buffer, m_{bc} is the mass of a buffer cell, $\boldsymbol{n_{bc}}$ is the number of cells and m_{EM} and m_{ICE} are the masses of the EM and ICE.

2.4.2 Series powertrain

The power balance equations for the series powertrain (illustrated in Figure 1.3(b)) can be described by

$$F_{dem}(\cdot)v_{dem}(t) = \boldsymbol{\tau_{EM}}(t)\frac{v_{dem}(t)}{R_w}\eta_{fg}^{\text{sign } F_{dem}(\cdot)} - \boldsymbol{P_{brk}}(t) \tag{2.9}$$

$$\boldsymbol{\tau_{EM}}(t)\frac{v_{dem}(t)}{R_w} + B_{EM}(\cdot) = \boldsymbol{P_b}(t) + \boldsymbol{P_c}(t)\eta_c(t) + \boldsymbol{P_{EGU}}(t) - P_{aux} \tag{2.10}$$

where $\boldsymbol{P_{EGU}}(t)$ is electric power delivered by the EGU and the rest of the variables are as described in Section 2.4.1.

Because the EGU is not mechanically connected to the wheels, it can be assumed that while turned on the EGU is operated in a narrow speed range and with small variations in speed. Therefore, the EGU inertia can be neglected and inertia of the powertrain components is simply the EM inertia, i.e.

$$J_p(\cdot) = J_{EM}. \tag{2.11}$$

The EGU losses may not be negligible during cranking, when the generator is used to start up the engine. A possible way to include these loses in the model has been described in Paper 2, where the cranking losses are considered to account with equivalent electric energy taken from the energy buffer.

The vehicle mass is described as

$$m(\cdot) = m_v + m_{EM} + m_{EGU} + \boldsymbol{n_{bc}}m_{bc} \tag{2.12}$$

where m_{EGU} is the mass of the EGU.

2.4.3 Series-parallel powertrain

The series-parallel powertrain can be described by combining the models of the parallel and the series powertrain. A model of this powertrain has been described in Paper 1, but in this section a slightly different model is given where the powertrain operation in series or parallel mode can be explicitly distinguished by the state of the clutch near the transmission. When the clutch is open, i.e. $\boldsymbol{c}(t) = 0$, this powertrain operates as a series powertrain,

and the ICE and EM1 can be represented as an EGU. When the clutch is closed, i.e. $\boldsymbol{c}(t) = 1$, the powertrain operates as a parallel powertrain. The power balance equations can then be described by

$$\begin{aligned} F_{dem}(\cdot)v_{dem}(t) = \boldsymbol{\tau_{EM2}}(t)\frac{v_{dem}(t)}{R_w}\eta_{fg2}^{\operatorname{sign} F_{dem}(\cdot)} - \boldsymbol{P_{brk}}(t) \\ + \boldsymbol{c}(t)\left(\boldsymbol{\tau_{EM1}}(t) + \boldsymbol{\tau_{ICE}}(t)\right)\frac{v_{dem}(t)}{R_w}\left(\eta_\gamma(\boldsymbol{\gamma}(t))\eta_{fg1}\right)^{\operatorname{sign} F_{dem}(\cdot)} \end{aligned} \tag{2.13}$$

$$\begin{aligned} \boldsymbol{c}(t)\left(\boldsymbol{\tau_{EM1}}(t)\frac{v_{dem}(t)}{R_w} + B_{EM1}(\cdot)\right) + \boldsymbol{\tau_{EM2}}(t)\frac{v_{dem}(t)}{R_w} + B_{EM2}(\cdot) \\ = \boldsymbol{P_b}(t) + \boldsymbol{P_c}(t)\eta_c(t) + (1 - \boldsymbol{c}(t))\,\boldsymbol{P_{EGU}}(t) - P_{aux}. \end{aligned} \tag{2.14}$$

where η_{fg1} and η_{fg2} denote the efficiencies of the final gears on the front and rear wheels axles, respectively. This way of modeling gives a closer connection to the series and parallel powertrain used in convex optimization in Paper 2.

When the clutch is closed the EM1 and ICE speed is determined by the wheels speed and the decision variables for these components are the torques $\boldsymbol{\tau_{EM1}}(t)$ and $\boldsymbol{\tau_{ICE}}(t)$. When the clutch is open, the EM1 and ICE speed is independent of the wheels speed and decision variable is the generated electric power $\boldsymbol{P_{EGU}}(t)$.

The inertia of the powertrain components can be computed as

$$J_p(\cdot) = \boldsymbol{c}(t)\left(J_{EM1} + J_{ICE}\right)r_\gamma^2(\boldsymbol{\gamma}(t)) + J_\gamma(\boldsymbol{\gamma}(t)) + J_{EM2} \tag{2.15}$$

with J_{EM1}, J_{EM2} and J_{ICE} denoting the inertia of the EM1, EM2 and ICE, respectively.

The vehicle mass is described as

$$m(\cdot) = m_v + m_{EM1} + m_{EM2} + m_{ICE} + \boldsymbol{n_{bc}}m_{bc} \tag{2.16}$$

with m_{EM1}, m_{EM2} and m_{ICE} denoting the mass of the EM1, EM2 and ICE, respectively.

2.4.4 Internal combustion engine (ICE)

The ICE is modeled with static losses $B_{ICE}(\cdot)$ which are typically given in a torque-speed map (for illustrative purposes, the left plot in Figure 2.2 depicts the ICE efficiency). The fuel power consumed by the ICE is then described by

$$P_f(\cdot) = \omega_{ICE}(\cdot)\boldsymbol{\tau_{ICE}}(t) + B_{ICE}(\cdot) \tag{2.17}$$

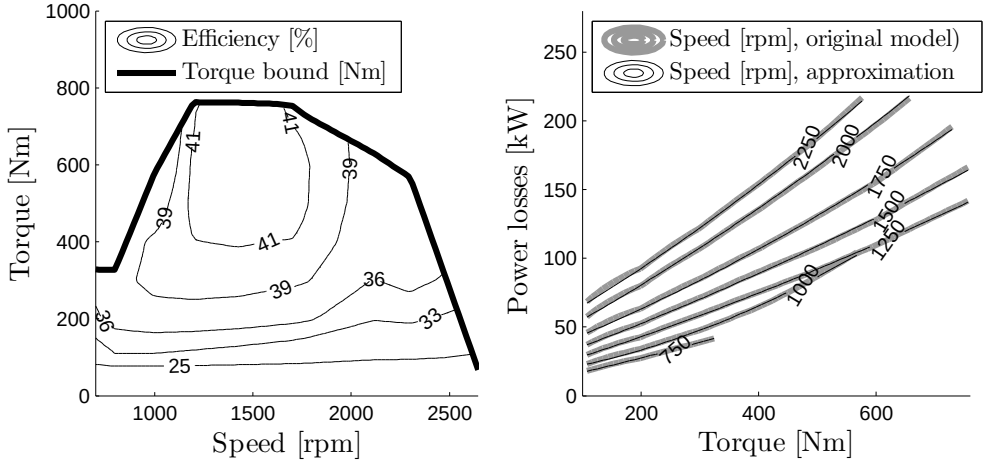

Figure 2.2: Left plot: static efficiency map of the ICE. Right plot: power losses of the original ICE model and approximation with quadratic losses for several ICE speeds.

where $\omega_{ICE}(\cdot)$ and $\boldsymbol{\tau_{ICE}}(t)$ are the ICE speed and torque, respectively. The ICE speed is directly related to the demanded vehicle speed by

$$\omega_{ICE}(\cdot) = v_{dem}(t)\frac{r_\gamma(\boldsymbol{\gamma}(t))r_{fg}}{R_w} \tag{2.18}$$

where it has been considered a transmission between the ICE and the wheels.

Both the ICE speed and torque are limited by

$$\omega_{ICE}(\cdot) \in [0, \omega_{ICEmax}] \tag{2.19}$$

$$\boldsymbol{\tau_{ICE}}(t) \in [0, \tau_{ICEmax}(\omega_{ICE}(\cdot))] \tag{2.20}$$

considering that no mechanical power is generated when the ICE is idling or off.

The losses are commonly approximated by affine or quadratic relations, also known as Willans lines [66, 67]. The approximation is a fairly accurate representation of actual engine data and has been verified on many different types of engines, from conventional spark ignition to compression ignition direct injection [59, 60]. An example of approximation with quadratic losses

$$B_{ICE}(\cdot) = c_0(\omega_{ICE}(\cdot))\boldsymbol{\tau_{ICE}^2}(t) + c_1(\omega_{ICE}(\cdot))\boldsymbol{\tau_{ICE}}(t) + c_2(\omega_{ICE}(\cdot))\boldsymbol{e_{on}}(t) \tag{2.21}$$

is given in the right plot of Figure 2.2. The coefficients $c_j(\omega_{ICE}(\cdot)), j = 0, 1, 2$, are found by least squares for a number of grid points of $\omega_{ICE}(\cdot)$. For

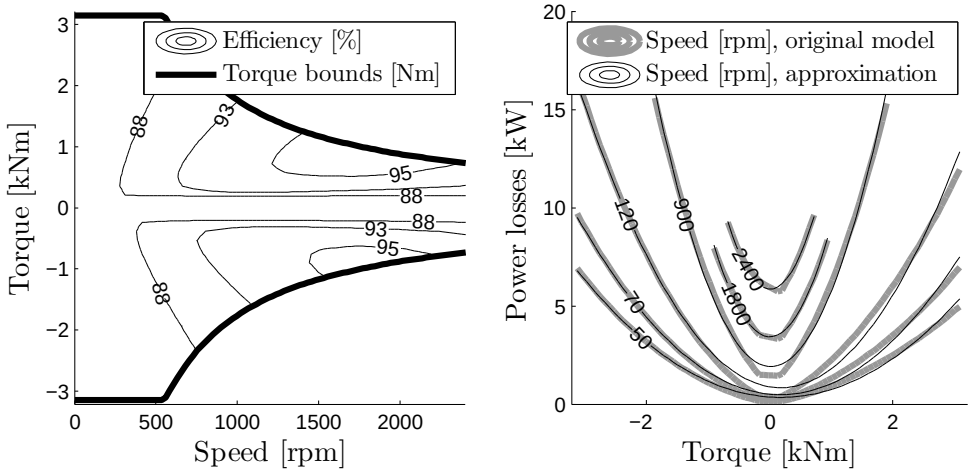

Figure 2.3: Left plot: static efficiency map of the EM. Right plot: power losses of the original EM model and approximation with quadratic losses for several EM speeds.

speed values not belonging to the grid nodes, the coefficients are obtained by linear interpolation. The approximated model requires an additional binary control signals $\boldsymbol{e_{on}}(t)$ that is needed to remove the idling losses $c_2(\omega_{ICE}(\cdot))$ when the engine is off.

To prevent frequent engine turn-ons that may result from the optimal control due to the lack of dynamics in the ICE model, it can be considered that during cranking (each time the ICE is turned on with the help of the EM), a certain amount of electric energy is consumed from the buffer. This is further described in Paper 2.

2.4.5 Electric machine (EM)

The EM is modeled with static losses $B_{EM}(\cdot)$ that relate the electrical power

$$P_{EMel}(\cdot) = \omega_{EM}(\cdot)\boldsymbol{\tau_{EM}}(t) + B_{EM}(\cdot) \tag{2.22}$$

to the mechanical power $\omega_{EM}(\cdot)\boldsymbol{\tau_{EM}}(t)$. The EM speed $\omega_{EM}(\cdot)$ and torque $\boldsymbol{\tau_{EM}}(t)$ are limited by

$$\omega_{EM}(t) \in [0, \omega_{EMmax}] \tag{2.23}$$

$$\boldsymbol{\tau_{EM}}(t) \in [\tau_{EMmin}(\omega_{EM}(t)), \tau_{EMmax}(\omega_{EM}(t))] \tag{2.24}$$

where $\omega_{EM}(t)$ is uniquely determined from the vehicle speed

$$\omega_{EM}(t) = v_{dem}(t)\frac{r_\gamma(\boldsymbol{\gamma}(t))r_{fg}}{R_w}. \tag{2.25}$$

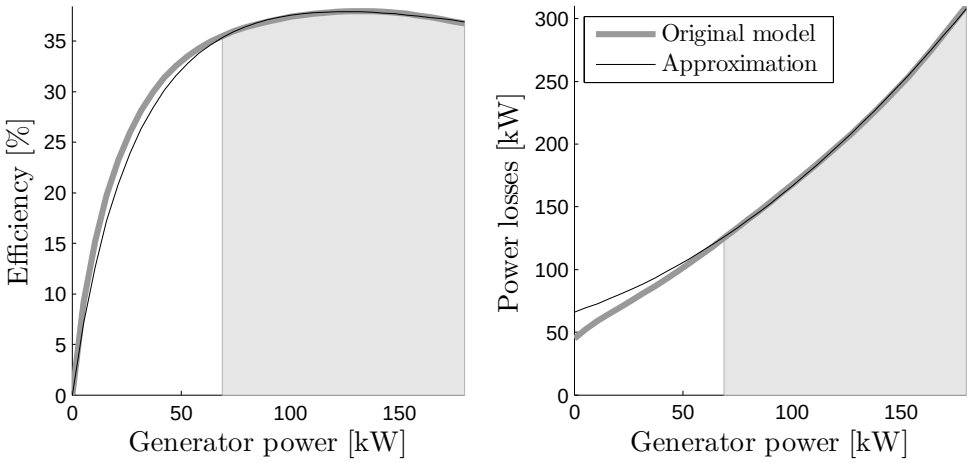

Figure 2.4: Efficiency, left plot, and power losses, right plot, of the EGU. Quadratic approximation of the power losses gives good fit within the shaded region.

Similarly as with the ICE, the EM losses can be approximated as quadratic

$$B_{EM}(\cdot) = b_0(\omega_{EM}(\cdot))\boldsymbol{\tau}_{\boldsymbol{EM}}^{\boldsymbol{2}}(t) + b_1(\omega_{EM}(\cdot))\boldsymbol{\tau}_{\boldsymbol{EM}}(t) + b_2(\omega_{EM}(\cdot)) \quad (2.26)$$

with speed dependent coefficients $b_j(\omega_{ICE}(\cdot)), j = 0, 1, 2$. An example of original and approximated EM model is given in Figure 2.3.

2.4.6 Engine-generator unit (EGU)

The EGU model can be described by combining the models of the ICE and EM, with static losses described by a torque-speed map. However, because the EGU is not mechanically connected to the wheels, its speed can be freely chosen to minimize the EGU losses for a required generator power $\boldsymbol{P}_{\boldsymbol{EGU}}(t)$. Then, the consumed fuel power by the EGU can be described as

$$P_f(\cdot) = \boldsymbol{P}_{\boldsymbol{EGU}}(t) + B_{EGU}(\cdot) \quad (2.27)$$

where the losses $B_{EGU}(\cdot)$ are given by a one-dimensional static map, or by a comprehensive mathematical model

$$B_{EGU}(\cdot) = P_f(\cdot)\left(1 - \eta_1\left(1 - e^{-\beta_1(P_f(\cdot) - P_{idle})}\right) - \eta_2 e^{-\beta_2(P_f(\cdot) - P_f^*)^2}\right) \quad (2.28)$$

that captures the essential EGU characteristics and compares reasonably well to manufacturer data [68]. Due to internal friction, the efficiency approaches zero at power lower than P_{idle}. Then, as $P_f(\cdot)$ increases, the efficiency increases with rate β_1 to a value close to η_1. The maximum EGU

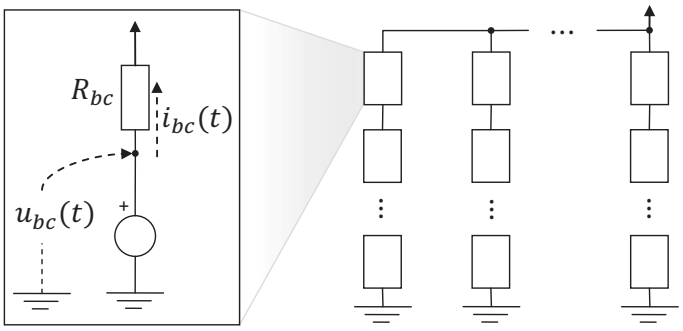

Figure 2.5: Equivalent battery circuit. The model of the battery cell is illustrated in the left side. The battery pack (right side) consists of parallel strings, with each string containing equal number of identical cells connected in series.

efficiency is about $\eta_1 + \eta_2$ centered on the fuel power P_f^* with highest efficiency. The parameter β_2 determines the bulginess of the efficiency peak. Low β_2 value gives flatter curve around P_f^*, while higher β_2 gives a prominent peak.

In this thesis the losses are approximated as quadratic

$$B_{EGU}(\cdot) = a_0 \boldsymbol{P}_{\boldsymbol{EGU}}^{\boldsymbol{2}}(t) + a_1 \boldsymbol{P}_{\boldsymbol{EGU}}(t) + a_2 \boldsymbol{e}_{\boldsymbol{on}}(t) \tag{2.29}$$

which give good fit for high generator power, see Figure 2.4. The approximation can be justified because the EGU will be mainly operated with high power, where the efficiency is high. Further discussion on this topic can be found in Paper 2.

2.4.7 Battery

The battery pack consists of identical cells equally divided in parallel strings, with the strings consisting of cells connected in series (Figure 2.5). Using a cell model with simple resistive circuit, as illustrated in Figure 2.5, the pack power can be computed as

$$\boldsymbol{P}_{\boldsymbol{b}}(t) = \left(u_{bc}(\cdot) i_{bc}(t) - R_{bc}\, i_{bc}^2(t)\right) \boldsymbol{n}_{\boldsymbol{bc}}. \tag{2.30}$$

In this equation $\boldsymbol{n}_{\boldsymbol{bc}}$ is the total number of cells in the pack, and $u_{bc}(\cdot)$, $i_{bc}(t)$ and R_{bc} are the open circuit voltage, current and resistance of each cell. Then, the power of each cell $\boldsymbol{P}_{\boldsymbol{b}}(t)/\boldsymbol{n}_{\boldsymbol{bc}}$ is identical and does not depend on the configuration of cells (series/parallel), but rather on the total number of cells in the pack. Therefore, in this thesis the problem of battery sizing focuses only on determining the total number of cells in the pack.

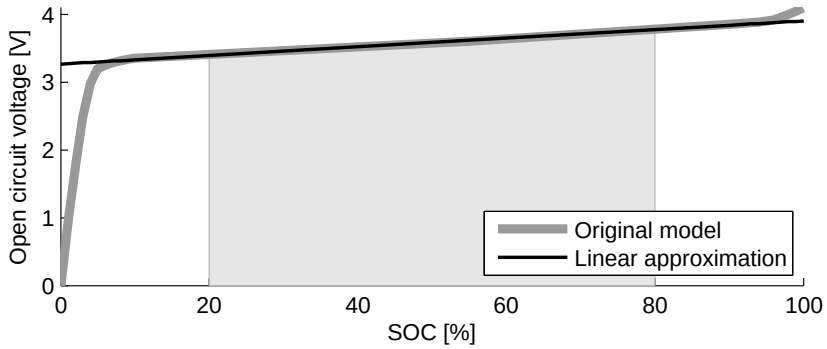

Figure 2.6: Model of the battery open circuit voltage and linear voltage-SOC approximation. Good fit is expected in the allowed SOC range represented by the shaded region.

In the optimization problem $\boldsymbol{n_{bc}}$ has a real value that indicates the total pack capacity. It can be expected that rounding this variable to the nearest integer gives small error if results point to large number of cells. This will generally be the case if the cells are chosen small.

From (2.30) the cell current can be described as

$$i_{bc}(\cdot) = \frac{1}{2R_{bc}} \left(u_{bc}(\cdot) - \sqrt{u_{bc}^2(\cdot) - \frac{4R_{bc}\boldsymbol{P_b}(t)}{\boldsymbol{n_{bc}}}} \right) \tag{2.31}$$

which can then be used in the battery dynamics equation

$$\boldsymbol{\dot{soc}_b}(t) = -\frac{1}{Q_{bc}} i_{bc}(\cdot). \tag{2.32}$$

Here $\boldsymbol{soc_b}(t)$ denotes the battery state of charge (SOC) and Q_{bc} is the cell capacity in [Ah]. It is considered that the cell current is positive when discharging the battery and negative otherwise. Both, the SOC and the cell current are limited by

$$\boldsymbol{soc_b}(t) \in [soc_{bmin}, soc_{bmax}] \tag{2.33}$$

$$i_{bc}(\cdot) \in [i_{bcmin}, i_{bcmax}] \tag{2.34}$$

where (2.33) is imposed to extend the battery cycle and calendar life. In HEVs the allowed SOC range is typically less than 20 %, and it can be extended to about 60 % in PHEVs [69].

Additional possible constraints are starting at desired SOC value, pre-

serving charge sustain operation, or limiting the Ah-throughput of the cell

$$\boldsymbol{soc_b}(t_0) = soc_{b0} \tag{2.35}$$

$$\boldsymbol{soc_b}(t_0) = \boldsymbol{soc_b}(t_f) \tag{2.36}$$

$$\int_{t_0}^{t_f} |i_{bc}(\cdot)|dt \leq Q_{Ah} \tag{2.37}$$

with t_0 and t_f denoting the initial and final time of the driven cycle. The Ah-throughput Q_{Ah} associated to the driven cycle is obtained by multiplying the length of the cycle with the maximum allowed Ah-throughput Q_{Ahmax} in the entire battery cell life of L_{bc} years, normalized per kilometer. Denoting by d the average distance traveled by the vehicle in one year, Q_{Ah} can be computed as

$$Q_{Ah} = \frac{\int_{t_0}^{t_f} v_{dem}(t)dt}{L_{bc}d} Q_{Ahmax}. \tag{2.38}$$

The cell open circuit voltage is a nonlinear function of SOC, as in Figure 2.6. For certain battery types, used in Paper 2 and 5, approximation can be used with constant voltage within the allowed SOC range. For battery types as in Figure 2.6, a better approximation is an affine function

$$u_{bc}(\cdot) = d_0 \boldsymbol{soc_b}(t) + d_1 \tag{2.39}$$

that gives good fit within the allowed SOC range. This is further discussed in Paper 3 and 4.

2.4.8 Ultracapacitor

Similar to the battery, the ultracapacitor pack consists of identical cells connected in parallel and series configuration. Likewise, the cell current is limited by

$$i_{uc}(\cdot) = \frac{1}{2R_{uc}} \left(\boldsymbol{u_{uc}}(t) - \sqrt{\boldsymbol{u_{uc}^2}(t) - \frac{4R_{uc}\boldsymbol{P_u}(t)}{\boldsymbol{n_{uc}}}} \right) \in [i_{ucmin}, i_{ucmax}] \tag{2.40}$$

where $\boldsymbol{P_u}(t)$ is the pack power, $\boldsymbol{n_{uc}}$ is the total number of cells in the pack, and $i_{uc}(\cdot)$, $\boldsymbol{u_{uc}}(t)$ and R_{uc} are the current, open circuit voltage and inner resistance of each cell, respectively. The cell dynamics are described by the open circuit voltage

$$\dot{\boldsymbol{u}}_{\boldsymbol{uc}}(t) = -\frac{1}{C_{uc}} i_{uc}(\cdot) \tag{2.41}$$

with C_{uc} denoting the cell capacity in [F]. The cell constraints may include an upper limit on the cell voltage u_{ucmax}, a constraint for starting at desired SOC value and preserving charge sustain operation, yielding

$$\boldsymbol{u_{uc}}(t) \in [0,1]u_{ucmax} \tag{2.42}$$
$$\boldsymbol{u_{uc}}(t_0) = u_{ucmax}soc_{u0} \tag{2.43}$$
$$\boldsymbol{u_{uc}}(t_f) = \boldsymbol{u_{uc}}(t_0). \tag{2.44}$$

The SOC of the ultracapacitor is here found as $soc_u = \boldsymbol{u_{uc}}(t)/u_{ucmax}$.

The essential difference between ultracapacitors and batteries is that ultracapacitors have higher power density, lower energy density, and can be utilized in the entire SOC range without a significant impact on the calendar life. Therefore, ultracapacitors can be operated at a low SOC where the maximum cell power is not at the maximum cell current i_{ucmax}, but at a lower current for which it holds

$$\frac{\partial \boldsymbol{P_u}(t)}{\partial i_{uc}(\cdot)} = 0 \Rightarrow i_{uc}(\cdot) = \frac{\boldsymbol{u_{uc}}(t)}{2R_{uc}} \Rightarrow \frac{P_{umax}}{\boldsymbol{n_{uc}}} = \frac{\boldsymbol{u_{uc}^2}(t)}{4R_{uc}}. \tag{2.45}$$

The cell power bounds can then be summarized as

$$\frac{\boldsymbol{P_u}(t)}{\boldsymbol{n_{uc}}} \geq \boldsymbol{u_{uc}}(t)i_{ucmin} - R_{uc}i_{ucmin}^2 \tag{2.46}$$
$$\frac{\boldsymbol{P_u}(t)}{\boldsymbol{n_{uc}}} \leq \begin{cases} \boldsymbol{u_{uc}}(t)i_{ucmax} - R_{uc}i_{ucmax}^2, & \boldsymbol{u_{uc}}(t) > 2R_{uc}i_{ucmax} \\ \boldsymbol{u_{uc}^2}(t)/(4R_{uc}), & \text{otherwise.} \end{cases} \tag{2.47}$$

An illustration of cell power bounds is depicted in Figure 2.7.

It is important to note that in HEV applications it is not common to operate ultracapacitors close to the peak power. This has been observed in Paper 3 and 4. Namely, in HEV applications ultracapacitors are sized by the energy storage requirement because of the relatively low energy density and the high power density [69, 70]. Hence, their optimal size is typically large enough to easily handle high power demands. Moreover, when operated at peak power, e.g. close to $\boldsymbol{u_{uc}^2}(t)/(4R_{uc})$, the efficiency is very low, i.e. close to 50 %. A more appropriate power is

$$\frac{\boldsymbol{P_u}(t)}{\boldsymbol{n_{uc}}} = \begin{cases} \eta_{uc}(1-\eta_{uc})\frac{\boldsymbol{u_{uc}^2}(t)}{R_{uc}}, & \boldsymbol{P_u}(t) \geq 0 \\ -\frac{1-\eta_{uc}}{\eta_{uc}^2}\frac{\boldsymbol{u_{uc}^2}(t)}{R_{uc}}, & \text{otherwise} \end{cases} \tag{2.48}$$

at which the efficiency is η_{uc}. Figure 2.7 illustrates a region with efficiency greater than or equal to 85 %.

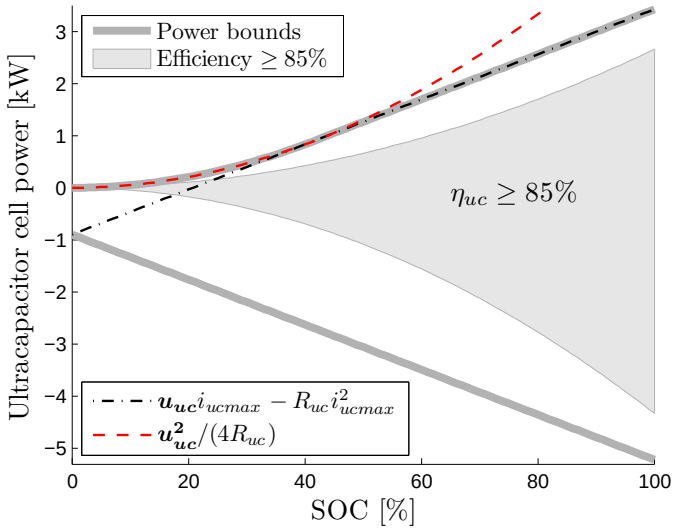

Figure 2.7: Bounds on the ultracapacitor cell power. In the shaded region the efficiency is above 85 %.

2.5 Thermal states

It has been shown in the previous section that the studied powertrain components have physical limits. The battery, for example, can be operated up to a certain maximum charging and discharging current, while the EM has limits on its motoring and generating torque. However, operating the components close to their physical limits cannot be maintained for longer time periods, without a risk of overheating and thereby damaging the components.

A simple way to prevent overheating of a vehicle component k, is to put an upper bound on its temperature $\boldsymbol{T_k}(t) \leq T_{kmax}$. Evidently, this requires that the vehicle component k, and perhaps some other components $j, j \neq k$, include temperature states $\boldsymbol{T_k}(t)$ and $\boldsymbol{T_j}(t)$, respectively. Then the change in temperature of the component k can be described by e.g. first order dynamics

$$C_{Tk}\dot{\boldsymbol{T}}_{\boldsymbol{k}}(t) = \sum_j \frac{\boldsymbol{T_j}(t) - \boldsymbol{T_k}(t)}{R_{Tj}} + B_k(\boldsymbol{u}(t)) - P_{kcool}(\boldsymbol{u}(t)) \tag{2.49}$$

which depends on the component's thermal capacitance C_{Tk} and the thermal resistance R_{Tj} of the medium between component k and the other components j (including the environment, i.e. ambient temperature). Moreover, the temperature increases with losses $B_k(\boldsymbol{u}(t))$ and may decrease with forced cooling $P_{kcool}(\boldsymbol{u}(t))$, both function of some control signals $\boldsymbol{u}(t)$.

An example of dimensioning a powertrain component under thermal constraints has been investigated in Paper 4.

2.6 Scaled ICE, EM and EGU models

Dimensioning powertrain components generally requires repeating the optimization with a set of component choices. (Exceptions are energy buffers where cells are clearly defined.) This is because powertrain components such as ICE, EM and EGU may differ significantly for different sizes. For example, the efficiency map of a two cylinder ICE is generally different than the efficiency map of a bigger ICE with four cylinders [67]. Yet, a common question in designing a cost effective HEV is to find the cost benefit from slightly changing the size of a component. A possible way to handle this without repeating the optimization too many times (if e.g. convex optimization is used), is to create few groups of significantly different component sizes, and to assume that the small variation of the component size within each of the groups does not change the efficiency map of the component. In each of these groups a typical component is chosen that is used as a baseline for comparing scaled components within the same group.

An example of baseline components, ICE, EM and EGU, are given in the left plots of Figure 2.8. It is assumed, for simplicity, that the torque and power losses of ICEs and EMs with different sizes, scale linearly with the torque and losses of the baseline components, while the speed range does not change [71]. Similarly, the generator power and the losses of EGUs with different sizes scale linearly with the generator power and losses of the baseline EGU. The torque/power of the scaled components can then be written as

$$\boldsymbol{\tau_{ICE}}(t) = \boldsymbol{s_{ICE}}\boldsymbol{\tau_{ICEb}}(t), \qquad B_{ICE}(\cdot) = \boldsymbol{s_{ICE}}B_{ICEb}(\cdot) \tag{2.50}$$

$$\boldsymbol{\tau_{EM}}(t) = \boldsymbol{s_{EM}}\boldsymbol{\tau_{EMb}}(t), \qquad B_{EM}(\cdot) = \boldsymbol{s_{EM}}B_{EMb}(\cdot) \tag{2.51}$$

$$\boldsymbol{P_{EGU}}(t) = \boldsymbol{s_{EGU}}\boldsymbol{P_{EGUb}}(t), \qquad B_{EGU}(\cdot) = \boldsymbol{s_{EGU}}B_{EGUb}(\cdot) \tag{2.52}$$

where $\boldsymbol{s_{ICE}}$, $\boldsymbol{s_{EM}}$ and $\boldsymbol{s_{EGU}}$ are decision variables denoting component sizes. The symbol b in the subscript stands for the baseline components. An example of scaled components is illustrated in the right plots of Figure 2.8.

The components mass and inertia can be also assumed to scale linearly, while the cost can be represented by an affine relation that gives a possibility to assign an initial cost for installing a component regardless of its size. Then, the mass, inertia and cost of a scaled component

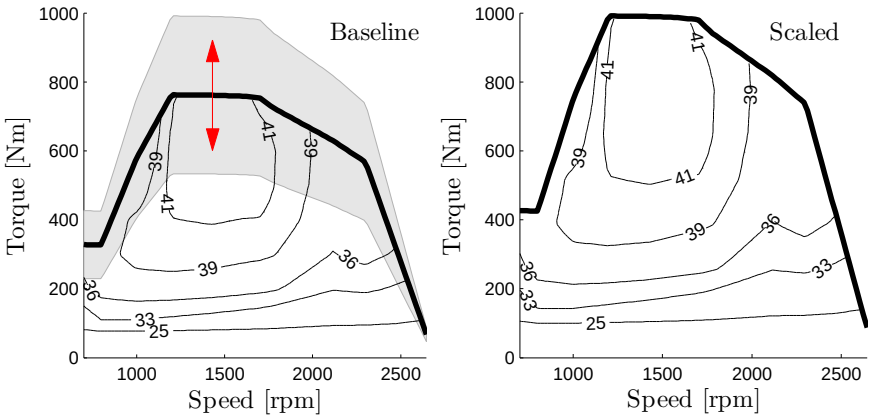

(a) ICE.

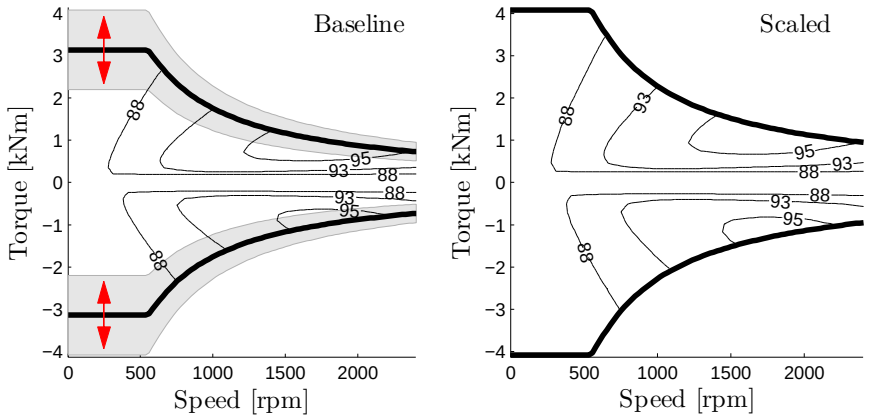

(b) EM.

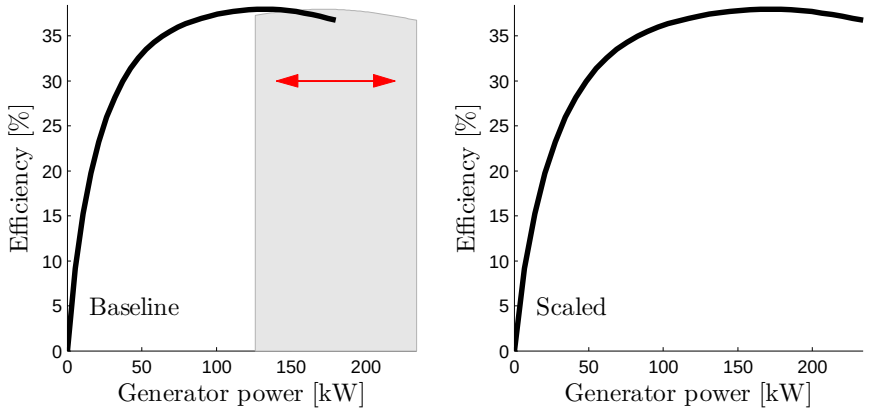

(c) EGU.

Figure 2.8: Dimensioning the powertrain components. The left plots show the baseline components. Components with different sizes may have torque or power bounds within the shaded region. The right plots show examples of scaled components with maximum allowed size.

$j \in \{ICE, EM, EGU\}$ is

$$m_j = \boldsymbol{s_j} m_{jb} \tag{2.53}$$
$$J_j = \boldsymbol{s_j} J_{jb} \tag{2.54}$$
$$C_j = C_{j0} + \boldsymbol{s_j} C_{jb} \tag{2.55}$$

where C_{j0} is initial cost for component j. An example of optimal sizing of an EGU in a PHEV bus is given in Paper 4, while sizing of ICE and EM using convex optimization has been performed in a recently submitted article [72].

Chapter 3

Optimization methods

This chapter gives an overview of the optimization methods used in the papers for solving the problem formulated in Section 2.1. A special attention is given to convex optimization, because this method has been used in all the papers, except Paper 1. The typical convex modeling steps used in Paper 2-5 are here explained through a simple example of battery sizing of a series HEV powertrain. A detailed explanation is given on why the remodeled convex problem points to the same solution of the original non-convex problem.

3.1 Optimization problem, revisited

The optimization objective, recall Section 2.1, is minimizing operational and components' cost for an HEV driven along a known driving cycle. If the vehicle has a plug-in connecter, then except fuel cost, the operational cost may also include a cost for consumed electricity on the driven cycle. The components' cost, e.g. for a vehicle based on a series powertrain topology, may include a cost for a battery, EGU and EM. The costs are expressed in a single objective

$$\int_{t_0}^{t_f} \left(w_f P_f(\cdot) + w_c \boldsymbol{P_c}(t)\right) dt + w_{bc} \boldsymbol{n_{bc}} + w_{EGU} \boldsymbol{s_{EGU}} + w_{EM} \boldsymbol{s_{EM}} \qquad (3.1)$$

using coefficients w_f, w_c in [currency/kWh], for fuel and electricity, respectively, and w_j in [currency], with j standing for a battery cell, EGU, and EM, respectively. The optimization is subject to constraints, discussed in Chapter 2, invoked by the driving cycle and the powertrain model. Decision variables are marked in bold in Chapter 2.

The coefficients $w_j, j \in \{bc, EGU, EM\}$ in (3.1) can be obtained from known components' prices C_j [currency], by considering that the payment

for a component j is divided in equal amounts over a period of y_j years with p_j percent yearly interest rate. Then, the equivalent components' cost related to the driven cycle is obtained by multiplying the length of the cycle with the components' price per kilometer, obtained by dividing with the average distance traveled by the vehicle in the component's life length of L_j years. If the vehicle travels in average d kilometers in one year, this yields

$$w_j = C_j \left(1 + p_j \frac{y_j + 1}{2}\right) \frac{\int_{t_0}^{t_f} v_{dem}(t)dt}{L_j d}, \quad j \in \{bc, EGU, EM\}. \tag{3.2}$$

3.2 Dynamic Programming

A possible approach for solving the powertrain dimensioning and control problem is by using Dynamic Programming (DP). DP is a well-known optimal control method that is widely used for HEV powertrain assessment and sizing, with high amount of academic literature and dedicated solvers to speed up computation time [73, 74, 75]. The algorithm uses Bellman's principle of optimality [33] to solve the problem via backwards recursion handling nonlinearities and constraints in a straightforward way. DP is capable of solving non-convex, mixed-integer problems, but its computation time, even when using dedicated solvers, increases exponentially with the number of state variables.

DP has been used in Paper 1 for assessment of HEV powertrains with fixed powertrain components, while for the powertrain sizing problem, in Paper 2 and 5, DP has been used as a benchmark to compare the solution from convex optimization of powertrain models with low complexity.

3.3 Convex optimization

This section gives a brief overview on convex optimization, used for solving the powertrain sizing and control problem in Paper 2-5. The notation is adopted from [61] with dom f meaning domain of f and $\mathbb{R}$ denoting the set of real numbers.

3.3.1 Convex sets, functions and problems

Definition 1. A set $\mathcal{C} \subseteq \mathbb{R}^n$ is convex if the line segment between any two points $\boldsymbol{x}, \boldsymbol{y} \in \mathcal{C}$ lies in $\mathcal{C}$, i.e. $\theta\boldsymbol{x} + (1-\theta)\boldsymbol{y} \in \mathcal{C}$ for any θ with $0 \leq \theta \leq 1$.

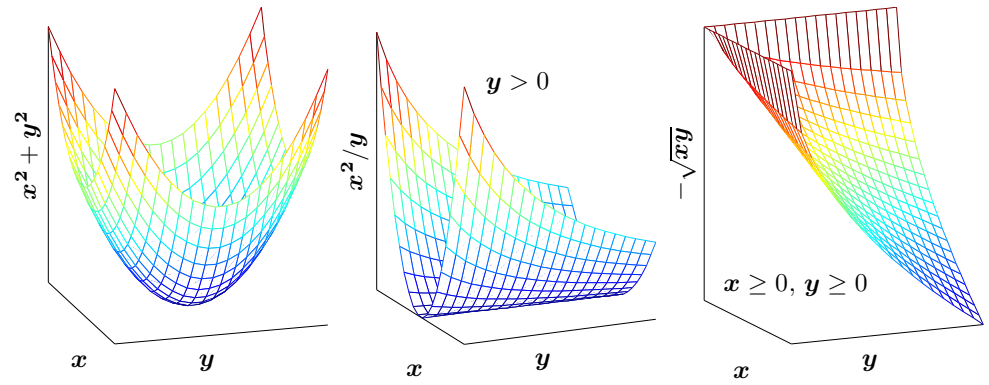

Figure 3.1: Convex functions.

Definition 2. A function $f : \mathbb{R}^n \to \mathbb{R}$ is convex if $\operatorname{dom} f$ is a convex set and $f(\theta \boldsymbol{x} + (1-\theta)\boldsymbol{y}) \leq \theta f(\boldsymbol{x}) + (1-\theta) f(\boldsymbol{y})$ for all $\boldsymbol{x}, \boldsymbol{y} \in \operatorname{dom} f$ and any θ with $0 \leq \theta \leq 1$.

The function f is said to be concave if $-f$ is convex. Some examples of convex functions are given in Figure 3.1.

Definition 3. The problem

$$\begin{aligned} \text{minimize} \quad & f_0(\boldsymbol{x}) \\ \text{subject to} \quad & f_i(\boldsymbol{x}) \leq 0, \quad i = 1, ..., m \\ & h_j(\boldsymbol{x}) = 0, \quad j = 1, ..., p \\ & \boldsymbol{x} \in \mathcal{X} \end{aligned}$$

is convex if $\mathcal{X} \subseteq \mathbb{R}^n$ is convex set, $f_i(\boldsymbol{x}), i = 0, ..., m$ are convex and $h_j(\boldsymbol{x}), j = 1, ..., p$ are affine in the decision variables $\boldsymbol{x}$.

3.3.2 Elementary convex functions

This thesis uses the methodology of disciplined convex programming [61], where convexity of complex functions is verified using operations that preserve convexity of elementary convex functions. The elementary convex (concave) functions, that have been used in Paper 2-5, are described by the following remarks that can be obtained directly from Definition 2.

Remark 1. An affine function $f(\boldsymbol{x}) = q\boldsymbol{x} + r$ is both convex and concave.

Remark 2. A quadratic function $f(\boldsymbol{x}) = p\boldsymbol{x}^2 + q\boldsymbol{x} + r$ with $\operatorname{dom} f \subseteq \mathbb{R}$ is convex if $p \geq 0$.

Remark 3. A quadratic-over-linear function $f(\boldsymbol{x}, \boldsymbol{y}) = \boldsymbol{x^2}/\boldsymbol{y}$ with $\operatorname{dom} f = \{(\boldsymbol{x}, \boldsymbol{y}) \in \mathbb{R}^2 \,|\, \boldsymbol{y} > 0\}$ is convex.

Remark 4. A function $f(\boldsymbol{x}, \boldsymbol{y}) = \sqrt{\boldsymbol{xy}}$ (a geometric mean of two elements) with $\operatorname{dom} f = \{(\boldsymbol{x}, \boldsymbol{y}) \in \mathbb{R}^2 \,|\, \boldsymbol{x} \geq 0, \boldsymbol{y} \geq 0\}$ is concave.

Remark 5. A product $f(\boldsymbol{x}, \boldsymbol{y}) = \boldsymbol{xy}$ is generally not a convex function.

3.3.3 Operations that preserve convexity

The following theorems, which proof can be found in [61], describe some of the operations that preserve convexity of sets and functions.

Theorem 1. *An intersection $\mathcal{S} = \bigcap \mathcal{S}_i$, of convex sets $\mathcal{S}_i$, is a convex set.*

Theorem 2. *A nonnegative weighted sum $f = \sum w_i f_i$ with $w_i \geq 0$, of convex functions f_i, is a convex function.*

This property can be extended to infinite sums and integrals. For example if $f(\boldsymbol{x}, y)$ is convex in $\boldsymbol{x}$ for each $y \in \mathcal{A}$, then $g(\boldsymbol{x}) = \int_{\mathcal{A}} w(y) f(\boldsymbol{x}, y) dy$ is convex in $\boldsymbol{x}$ if $w(y) \geq 0$.

Theorem 3. *A pointwise maximum $f(\boldsymbol{x}) = \max\{f_1(\boldsymbol{x}), ..., f_m(\boldsymbol{x})\}$, of convex functions $f_i(\boldsymbol{x}), i = 1, ..., m$, is a convex function.*

Similarly, a pointwise minimum $f(\boldsymbol{x}) = \min\{f_1(\boldsymbol{x}), ..., f_m(\boldsymbol{x})\}$, of concave functions $f_i(\boldsymbol{x}), i = 1, ..., m$, is a concave function.

3.3.4 Heuristic decisions

A limitation of convex optimization is that integer decision variables are not allowed as the set of integer numbers is not convex. The powertrain sizing and control problem includes a binary variable for controlling the ICE on/off state and an integer variable for controlling transmission gear at the parallel and combined powertrains. The approach taken in this thesis is to decide the integer variables by heuristics, and to remodel (or approximate) the remaining problem as a convex sub-problem.

In this case, the heuristics serves two purposes: it removes the need for solving a mixed integer problem; and at the same time it allows for a flexible approach to model the performance of the gearshift strategy which makes it possible to incorporate both physical constraints and limitations imposed by drivability considerations.

Heuristic decisions based on demanded power and speed have been proposed in Paper 2, where it has been shown that although the convex modeling approximations have small influence on the optimal result, the influence

from gear heuristics is more visible and deserves further attention. A more detailed study on the sensitivity of the ICE on/off heuristics has been considered in Paper 5, where it has been observed that the error due to on/off heuristics at series powertrains is below 1 %, even for a simple heuristic rule that turns the ICE on for power demands exceeding a certain threshold.

In order to further improve the heuristics a new strategy has been proposed in Paper 5, which practically reaches the global optimum of the mixed-integer problem (error below 0.03 %). Additional studies are needed to extend the method to gear selection heuristics.

3.3.5 Convex optimization method

After the integer variables are decided by heuristics, the remaining problem can be modeled as a convex sub-problem. The modeling steps include approximations with quadratic power losses, relaxations of equalities to inequalities, introduction of new decision variables, change of variables, etc. Details on the modeling steps for a reformulation of the original problem into a convex sub-problem can be found in Paper 2-5. The convex sub-problem can then be solved using generally available solvers, such as SeDuMi [76], or SDPT3 [77].

The engine on/off and gear heuristics (see Paper 2 and 5) may require the convex sub-problem to be solved in several nested loops. Then, the steps taken to solve the problem of powertrain sizing can be summarized as follows:

1. Define desired vehicle performance by deciding the driving cycle.
2. Define a charging infrastructure by deciding on charging stations, their distribution on the driving cycle and charging interval per station.
3. Loop 1: Decide the engine on/off state $e_{on}(t)$ using heuristics.
4. Loop 2 (for parallel and combined powertrains only): Decide transmission gear $\gamma(t)$ using heuristics.
5. In each iteration of the nested loops solve a convex sub-problem.

3.4 Convex modeling example

This section gives an example of optimal powertrain sizing and control of an HEV using convex optimization. The powertrain is in a series topology and it is assumed, for simplicity, that the only sizing component is an ultracapacitor.

The engine on/off control is decided prior to the optimization using heuristics that turn the engine on if the power of the vehicle without the weight of the ultracapacitor, $F_{dem}(\boldsymbol{n_{uc}} = 0, t)v_{dem}(t)$, exceeds a threshold P^*_{on}. This yields

$$e_{on}(t) = \begin{cases} 1, & F_{dem}(0,t)v_{dem}(t) > P^*_{on} \\ 0, & \text{otherwise.} \end{cases} \tag{3.3}$$

The optimal power threshold P^*_{on} is found by iteratively solving an optimization sub-problem (the problem in which $e_{on}(t)$ is predefined) for several values of P_{on} within the power range of the vehicle.

3.4.1 Non-convex sub-problem

The sub-problem minimizes fuel consumption and ultracapacitor cost subject to the powertrain constraints described in Section 2.4. It can be summarized as

$$\begin{aligned}
&\text{minimize} \\
&w_f \int_{t_0}^{t_f} \left(\boldsymbol{P_{EGU}}(t) + B_{EGU}(\cdot)\right) dt + w_{uc}\boldsymbol{n_{uc}} && (3.4)\\
&\forall t \in [t_0, t_f], \text{ subject to} \\
&F_{dem}(\boldsymbol{n_{uc}}, t)v_{dem}(t) = \boldsymbol{\tau_{EM}}(t)\frac{v_{dem}(t)}{R_w} - \boldsymbol{P_{brk}}(t) && (3.5)\\
&\boldsymbol{\tau_{EM}}(t)\frac{v_{dem}(t)}{R_w} + B_{EM}(\cdot) = \boldsymbol{P_u}(t) + \boldsymbol{P_{EGU}}(t) - P_{aux} && (3.6)\\
&\dot{\boldsymbol{u}}_{\boldsymbol{uc}}(t) = -\frac{1}{C_{uc}} i_{uc}(\cdot) && (3.7)\\
&\boldsymbol{u_{uc}}(t) \in [0,1]u_{ucmax} && (3.8)\\
&i_{uc}(\cdot) \in [i_{ucmin}, i_{ucmax}] && (3.9)\\
&\boldsymbol{P_{EGU}}(t) \in [0, e_{on}(t)P_{EGUmax}] && (3.10)\\
&\boldsymbol{\tau_{EM}}(t) \in [\tau_{EMmin}(\omega_{EM}(t)), \tau_{EMmax}(\omega_{EM}(t))] && (3.11)\\
&\boldsymbol{P_{brk}}(t) \geq 0 && (3.12)\\
&\boldsymbol{n_{uc}} \geq 0 && (3.13)
\end{aligned}$$

with optimization variables $\boldsymbol{P_{EGU}}(t)$, $\boldsymbol{P_u}(t)$, $\boldsymbol{P_{brk}}(t)$, $\boldsymbol{\tau_{EM}}(t)$, $\boldsymbol{u_{uc}}(t)$ and $\boldsymbol{n_{uc}}$. Recall from (2.4) and (2.12) that the demanded force $F_{dem}(\boldsymbol{n_{uc}}, t)$ is affine in $\boldsymbol{n_{uc}}$, the ultracapacitor cell current is given as

$$i_{uc}(\cdot) = \frac{1}{2R_{uc}} \left(\boldsymbol{u_{uc}}(t) - \sqrt{\boldsymbol{u_{uc}^2}(t) - \frac{4R_{uc}\boldsymbol{P_u}(t)}{\boldsymbol{n_{uc}}}} \right) \tag{3.14}$$

and the EM and EGU losses are approximated by quadratic functions in (2.26) and (2.29).

Even with approximations of the power losses and with $e_{on}(t)$ predefined, the optimization sub-problem is not convex. This is because the function (3.14) is not convex and the constraints (3.6) and (3.7) bind nonlinear functions with equality.

3.4.2 Convex modeling steps

The optimization sub-problem can be reformulated as convex without any further approximations. The function (3.14) used in (3.7) and (3.9) can be remodeled as convex by introducing a variable change, where instead of the cell open circuit voltage, the optimization variable is the pack energy

$$\boldsymbol{E_u}(t) = \frac{C_{uc}\boldsymbol{u_{uc}^2}(t)}{2}\boldsymbol{n_{uc}} \Rightarrow \dot{\boldsymbol{E}}_{\boldsymbol{u}}(t) = C_{uc}\boldsymbol{n_{uc}}\boldsymbol{u_{uc}}(t)\dot{\boldsymbol{u}}_{\boldsymbol{uc}}(t). \tag{3.15}$$

Then, a new optimization variable is introduced that depicts pack losses

$$\boldsymbol{B_u}(t) = R_{uc}i_{uc}^2(\cdot)\boldsymbol{n_{uc}} \tag{3.16}$$

which can be also written as

$$\boldsymbol{B_u}(t) = \frac{\boldsymbol{E_u}(t)}{R_{uc}C_{uc}} - \boldsymbol{P_u}(t) - \frac{1}{R_{uc}C_{uc}}\sqrt{\boldsymbol{E_u}(t)\left(\boldsymbol{E_u}(t) - 2R_{cu}C_{uc}\boldsymbol{P_u}(t)\right)} \tag{3.17}$$

after using (3.14) and (3.15) in (3.16). The reason for introducing the new variable $\boldsymbol{B_u}(t)$ is to easily explain the remaining convexifying steps. This procedure has been also used in Paper 4, while in Paper 3 convex modeling steps are shown without the need for $\boldsymbol{B_u}(t)$.

The right side of (3.17) is convex because it is a weighted sum (see Theorem 2) of affine functions $\boldsymbol{E_u}(t)/(R_{uc}C_{uc})$ and $\boldsymbol{P_u}(t)$, and a geometric mean (see Remark 4) of nonnegative affine functions $\boldsymbol{E_u}(t)$ and $\boldsymbol{E_u}(t) - 2R_{cu}C_{uc}\boldsymbol{P_u}(t)$. The nonnegativeness of the latter comes directly from (2.45). The last step that will make the constraint (3.17) convex is to relax the equality with $\geq$. Then, by moving $\boldsymbol{B_u}(t)$ on the right side of (3.17) a constraint is obtained in the general convex form

$$0 \geq -\boldsymbol{B_u}(t) + \frac{\boldsymbol{E_u}(t)}{R_{uc}C_{uc}} - \boldsymbol{P_u}(t) - \frac{1}{R_{uc}C_{uc}}\sqrt{\boldsymbol{E_u}(t)\left(\boldsymbol{E_u}(t) - 2R_{cu}C_{uc}\boldsymbol{P_u}(t)\right)}. \tag{3.18}$$

The relaxation changes the optimization problem as it allows for higher power losses than those corresponding to the used ultracapacitor power.

However, at the optimum (3.18) will be satisfied with equality, because there is no incentive for higher losses. Therefore, the solution of the relaxed problem will be optimal to the non-relaxed problem as well. Assume the contrary, if we suppose that for an optimal solution (3.18) holds with inequality, then the solution must have included some unnecessary losses. This means that it is possible to construct other state/control trajectory for which (3.18) will hold with equality and where these unnecessary losses will not be present. However, due to the fewer losses, there will be less need for using the EGU in delivering the power demand, and the total optimization cost will be lower. This means that the solution where (3.18) holds with inequality could not have been optimal. This technique of relaxing equality constraints to inequalities where the optimum gives equality has been extensively used in Paper 2-5. However, relaxing equality constraints cannot be used for all problems. For example, if the problem includes a constraint that does not allow usage of the buffer at cold start of the vehicle under low ambient temperature, then there could be an incentive for higher losses where (3.18) will hold with inequality. These losses could still give lower optimization cost than the realistic cost where (3.18) holds with equality.

After applying the variable change (3.14) in (3.15), the constraints (3.7) and (3.8) will change to

$$\dot{\boldsymbol{E}}_{\boldsymbol{u}}(t) = -(\boldsymbol{P}_{\boldsymbol{u}}(t) + \boldsymbol{B}_{\boldsymbol{u}}(t)) \tag{3.19}$$

$$\boldsymbol{E}_{\boldsymbol{u}}(t) \in [0, \frac{C_{uc} u_{ucmax}^2}{2} \boldsymbol{n}_{\boldsymbol{uc}}] \tag{3.20}$$

while the constraints on the cell current (3.9) can be written as constraints on the pack power (see also (2.46) and (2.47))

$$\boldsymbol{P}_{\boldsymbol{u}}(t) \geq i_{ucmin} \sqrt{\frac{2\boldsymbol{E}_{\boldsymbol{u}}(t)\boldsymbol{n}_{\boldsymbol{uc}}}{C_{uc}}} - R_{uc} i_{ucmin}^2 \boldsymbol{n}_{\boldsymbol{uc}} \tag{3.21}$$

$$\boldsymbol{P}_{\boldsymbol{u}}(t) \leq \min \left\{ i_{ucmax} \sqrt{\frac{2\boldsymbol{E}_{\boldsymbol{u}}(t)\boldsymbol{n}_{\boldsymbol{uc}}}{C_{uc}}} - \boldsymbol{B}_{\boldsymbol{u}}(t), \frac{\boldsymbol{E}_{\boldsymbol{u}}(t)}{2R_{uc}C_{uc}} \right\}. \tag{3.22}$$

The pointwise minimum of concave functions in (3.22) is concave by Theorem 3. This constraint can be also written as two inequality constraints, where $\boldsymbol{P}_{\boldsymbol{u}}(t)$ is less than or equal to the two terms in the min function. A more detailed derivation of (3.22) can be found in Paper 3.

Finally, the problem can be simplified by taking the braking power out of the optimization. The constraint (3.5) can be written as

$$\boldsymbol{\tau}_{\boldsymbol{EM}}(t) \geq R_w F_{dem}(\boldsymbol{n}_{\boldsymbol{uc}}, t) \tag{3.23}$$

or it can even be combined with the torque bound (3.11) giving the following constraints

$$\boldsymbol{\tau_{EM}}(t) \geq \max\left\{R_w F_{dem}(\boldsymbol{n_{uc}}, t), \tau_{EMmin}(\omega_{EM}(t))\right\} \tag{3.24}$$

$$\boldsymbol{\tau_{EM}}(t) \leq \tau_{EMmax}(\omega_{EM}(t)). \tag{3.25}$$

Excluding the braking power does not change the optimal result, since at the optimum (3.24) will hold with equality, except during braking when the vehicle cannot recuperate all the braking energy. Then, the remaining energy is dissipated at the friction brakes and the optimal braking power can be obtained after the optimization has finished from

$$\boldsymbol{P^*_{brk}}(t) = \boldsymbol{\tau^*_{EM}}(t)\frac{v_{dem}(t)}{R_w} - F_{dem}(\boldsymbol{n^*_{uc}}, t)v_{dem}(t) \tag{3.26}$$

with $*$ indicating the optimum value.

3.4.3 Convex sub-problem

The convex sub-problem, summarized from the previous section, can be written in discrete time as

minimize

$$w_f \sum_{0}^{N-1} \left(\boldsymbol{P_{EGU}}(k) + B_{EGU}(\cdot)\right) + w_{uc}\boldsymbol{n_{uc}} \tag{3.27}$$

$\forall k \in \{0, ..., N-1\},$ subject to

$$\boldsymbol{\tau_{EM}}(k)\frac{v_{dem}(k)}{R_w} + B_{EM}(\cdot) = \boldsymbol{P_u}(k) + \boldsymbol{P_{EGU}}(k) - P_{aux} \tag{3.28}$$

$$\boldsymbol{E_u}(k+1) = \boldsymbol{E_u}(k) - h(\boldsymbol{P_u}(k) + \boldsymbol{B_u}(k)) \tag{3.29}$$

$$\boldsymbol{E_u}(k) \in [0, \frac{C_{uc}u^2_{ucmax}}{2}\boldsymbol{n_{uc}}] \tag{3.30}$$

$$\boldsymbol{P_u}(k) \geq i_{ucmin}\sqrt{\frac{2\boldsymbol{E_u}(k)\boldsymbol{n_{uc}}}{C_{uc}}} - R_{uc}i^2_{ucmin}\boldsymbol{n_{uc}} \tag{3.31}$$

$$\boldsymbol{P_u}(k) \leq \min\left\{i_{ucmax}\sqrt{\frac{2\boldsymbol{E_u}(k)\boldsymbol{n_{uc}}}{C_{uc}}} - \boldsymbol{B_u}(k), \frac{\boldsymbol{E_u}(k)}{2R_{uc}C_{uc}}\right\} \tag{3.32}$$

$$\boldsymbol{P_{EGU}}(k) \in [0, e_{on}(k)P_{EGUmax}] \tag{3.33}$$

$$\boldsymbol{\tau_{EM}}(k) \geq \max\left\{R_w F_{dem}(\boldsymbol{n_{uc}}, k), \tau_{EMmin}(\omega_{EM}(k))\right\} \tag{3.34}$$

$$\boldsymbol{\tau_{EM}}(k) \leq \tau_{EMmax}(\omega_{EM}(k)) \tag{3.35}$$

$$\boldsymbol{n_{uc}} \geq 0 \tag{3.36}$$

with optimization variables $\boldsymbol{P_{EGU}}(k)$, $\boldsymbol{P_u}(k)$, $\boldsymbol{B_u}(k)$, $\boldsymbol{\tau_{EM}}(k)$, $\boldsymbol{E_u}(k)$ and $\boldsymbol{n_{uc}}$. The derivative (3.19) has been replaced with a first order forward Euler discretization with a sampling time h, giving N time samples for the chosen driving cycle. Before passing the problem to the solver (or first to the parser, see Paper 2 for details), the variables are scaled. For example, in the convex problem above the optimization variables can be scaled as $\boldsymbol{P_{EGU}}(k) = M_P\tilde{\boldsymbol{P}}_{\boldsymbol{EGU}}(k)$, $\boldsymbol{P_u}(k) = M_P\tilde{\boldsymbol{P}}_{\boldsymbol{u}}(k)$, $\boldsymbol{B_u}(k) = M_P\tilde{\boldsymbol{B}}_{\boldsymbol{u}}(k)$, $\boldsymbol{\tau_{EM}}(k) = M_T\tilde{\boldsymbol{\tau}}_{\boldsymbol{EM}}(k)$, $\boldsymbol{E_u}(k) = M_E\tilde{\boldsymbol{E}}_{\boldsymbol{u}}(k)$ and $\boldsymbol{n_{uc}} = M_N\tilde{\boldsymbol{n}}_{\boldsymbol{uc}}$, where the scaling parameters M_P, M_T, M_E and M_N are expected magnitudes that can be estimated from the power demanded by the driving cycle, the physical limits of the components, or by engineering conjecture.

3.5 Other optimal control techniques

Except DP and convex optimization, this thesis also uses another optimal control strategy based on moving the state equality constraints to the objective function of the optimization problem. The new extended objective, i.e. the Hamiltonian [78, 79], then includes weighted system dynamics, where the weighting factors are the Lagrange multipliers [80, 81] obtained directly from the Pontryagin's maximum principle [82]. This is a well-known strategy that has been extensively used for real-time control of HEVs [23, 65, 83, 84, 85, 86], but in this thesis, the Pontryagin's maximum principle has been used for improving the ICE on/off heuristics. The strategy is detailed in Paper 5 and requires a convex problem to be solved iteratively, while using the Hamiltonian to obtain an information on the possible improvement in cost from flipping the value of the engine on/off signal at certain time instances.

Chapter 4

Summary of included papers

This chapter provides a brief summary of the papers that constitute the base for this thesis. Full versions of the papers are included in Part II. The papers have been reformatted to increase readability and to comply with the layout of the rest of the thesis.

Paper 1

> N. Murgovski, J. Sjöberg, J. Fredriksson, A methodology and a tool for evaluating hybrid electric powertrain configurations, *Int. J. Electric and Hybrid Vehicles, vol. 3, no. 3, p. 219-245, 2011.*

Paper 1 describes a methodology for automatic optimization of hybrid electric powertrains. The methodology is developed and implemented in a tool, and the paper is written in the form of describing the tool. The tool can be used to estimate the potential of an HEV powertrain configuration without developing a real-time control algorithm. Inputs, such as dynamic vehicle model, driving cycle and optimization criterion, are given by the user and the tool first produces a simplified powertrain model in a form of static maps. The tool produces these maps automatically by performing a series of simulations of the dynamic model at gridded values of the input signals until steady state has been reached. Hence, the production of the maps includes long simulation and special measures are taken to not exaggerate this time. The optimization is based on Dynamic Programming [33], which is used to find an optimal power split that minimizes the chosen criterion.

The tool integrates the model simplification and optimization with a minimized need for interaction from the user. The user does not need to understand details of the model. Instead, parameter values for the algorithms are set automatically, although an experienced user can change some

of the parameters. The only requirement on the model is to provide access to some general variables and that it has a power split that can be fully controlled. This makes it possible to work with non-transparent models, e.g. models which are compiled, or hidden of intellectual property reasons.

Except describing the tool, the paper also describes solutions to a number of problems related to the goals, which are 1) automize the process as much as possible so that the need of user choices is reduced, and 2) limit the computational burden in the optimization. The solutions to these problems include a strategy to obtain maps for non-transparent vehicle models, automatic decision of the grid points for the maps, assessing the quality of the approximate maps, and a way to obtain map values although the model is not in equilibrium with regard to some states.

The paper presents two examples of powertrain evaluation, in terms of fuel consumption, for a parallel and a series-parallel powertrain.

Paper 2

> N. Murgovski, L. Johannesson, J. Sjöberg, B. Egardt, Component sizing of a plug-in hybrid electric powertrain via convex optimization, *J. Mechatronics, vol. 22, no. 1, p. 106-120, 2012.*

The methodology described in Paper 1 is useful for assessment of a fixed powertrain, but it has a limited use for dimensioning HEV powertrains. This is because the optimization needs to be repeated many times for different component sizes, and this may require very long computation time.

In order to lower the computational burden, Paper 2 presents a novel convex modeling approach which allows the problem of simultaneous optimization of battery size and energy management of a PHEV powertrain to be formulated as a semidefinite convex problem. This convex problem can then be efficiently solved for a global optimum using generally available solvers, SeDuMi [76], SDPT3 [77].

The studied powertrain belongs to a city bus, with either a series or a parallel topology, which is driven along a perfectly known bus line with a fixed charging infrastructure. In the optimization approach the power characteristics of the engine, the engine-generator unit and the electric machines are approximated by a convex second order polynomial, and the convex battery model assumes quadratic losses. The only heuristic choice in the optimization is the gear selection and the engine on/off operation which are tuned in an outer optimization loop.

The convexifying approximations are validated by comparing with results obtained by Dynamic Programming when using the original nonlinear,

non-convex, mixed-integer models. The comparison clearly shows the importance of the gear and engine on/off decisions, and it also shows that the convex optimization and Dynamic Programming point toward similar battery size and operating cost when the same gear and engine on/off heuristics are used.

Two examples illustrate the methodology of the optimal PHEV battery design for a bus line with fixed charging infrastructure. The first example investigates if the convex problem results in a similar battery design compared to the non-convex mixed integer problem solved by Dynamic Programming. The results indicate that both optimization problems point toward a similar solution. The second example studies a PHEV city bus equipped with a dual battery comprised of both energy optimized cells and power optimized cells; a problem that can be solved in minutes with the convex optimization approach, but would require a significant computational effort with the Dynamic Programming approach. Besides demonstrating the utility of the convex modeling approach the example clearly shows the sensitivity of battery sizing with respect to battery prices and charging power.

Paper 3

> N. Murgovski, L. Johannesson, J. Sjöberg, Convex modeling of energy buffers in power control applications, *Submitted to the IFAC Workshop on Engine and Powertrain Control, Simulation and Modeling (ECOSM), Rueil-Malmaison, France.*

Convex modeling steps for sizing batteries while optimally controlling an HEV have been proposed in Paper 2, where it has been shown that the error due to the convexifying approximations is small as long as the battery open circuit voltage is nearly constant within the operating State of Charge (SOC) interval. Due to this limitation the presented strategy is suitable only for certain battery types and not for ultracapacitors.

This paper is an extension of Paper 2 and shows modeling steps to allow for simultaneous sizing of ultracapacitors while optimally controlling HEVs via convex optimization techniques. Moreover, the proposed method also allows for sizing of batteries with nearly linear voltage-SOC dependency.

The convex modeling steps are described through a problem of optimal buffer sizing and control of a hybrid electric vehicle. The studied vehicle is a city bus driven along a perfectly known bus line, with an energy buffer that could be either a battery, or an ultracapacitor. Both the ultracapacitor and the battery are modeled with quadratic losses and the resulting convex problem is a semidefinite program [61].

The paper also shows modeling steps for alternative convex models where power losses and power limits of the energy buffer are approximated. By this, the computation time is decreased by up to 50 %, i.e. the computation time of the battery sizing problem is decreased from about 15 s to about 7.5 s in average, without an optimization error.

Paper 4

> N. Murgovski, L. Johannesson, A. Grauers, J. Sjöberg, Dimensioning and control of a thermally constrained double buffer plug-in HEV powertrain, *Submitted to the 51st IEEE Conference on Decision and Control, Maui, Hawaii.*

This paper describes modeling steps to enable fast dimensioning of powertrain components while optimally controlling a plug-in hybrid electric bus with a series powertrain topology. The components to be sized are engine-generator unit, and a double energy buffer consisting of a battery with nearly linear voltage-SOC dependency and a thermally constrained ultracapacitor. The model dynamics are described with three continuous states, two for the battery and ultracapacitor SOC and one for the ultracapacitor temperature. The powertrain components are modeled with quadratic losses and the resulting convex problem is a semidefinite program [61].

The paper also gives an example showing how the optimal sizes of the components are affected for two different charging scenarios. In the first scenario the bus can charge with 200 kW for a couple of seconds while standing still at bus stops, and in the second scenario the bus can charge for a couple of minutes before starting the route. The charger power in the second scenario is left for the optimization to find it.

Paper 5

> N. Murgovski, L. Johannesson, J. Sjöberg, Engine on/off control for dimensioning hybrid electric powertrains via convex optimization, *Submitted to the IEEE Transactions on Vehicular Technology.*

This paper proposes a novel heuristic strategy that decides the engine on/off control for PHEV powertrains. The method allows the problem to be solved using convex optimization techniques, where a solution near global optimum is obtained in a relatively short computation time, which may otherwise need very long time when solved by algorithms guaranteeing global optimum, such as Dynamic Programming.

The method is based on the Pontryagin's maximum principle [82] and requires the convex problem to be solved iteratively, while using the Hamiltonian [78, 79] to obtain an information on the possible improvement in cost from flipping the value of the engine on/off signal at certain time instances. The studied vehicle is a PHEV bus with a series topology which is driven along a perfectly known bus line with a fixed charging infrastructure. The bus can charge its battery ether at standstill, or while driving along a tram line.

The paper illustrates several examples where the problem of battery sizing, investigated for four different bus lines and two different battery types, is solved in less than 15 min. The results are validated with Dynamic Programming showing an error of less than 0.35 %. The problem of optimal control for a powertrain with a fixed battery is solved for 176 different battery sizes, each lasting less than 5 min, and each with an error of less than 0.03 %.

Chapter 5

Concluding remarks and future work

This chapter points out the strengths and weaknesses of the proposed methodology and discusses future challenges.

5.1 Dynamic Programming or convex optimization

This thesis uses both DP and convex optimization for dimensioning HEV powertrains, so this section discusses when is one algorithm more suitable than the other.

The main reason for using convex optimization is the relatively short computation time with regard to the number of states. Moreover, generic solvers and parsers exist, [76, 77, 87, 88], which allow the problems to be written in a very readable and easily extendable form. There is also vast amount of literature on both convex optimization and on techniques to distribute the optimization over several computers [89]. The drawback of using convex optimization is that it requires model approximations and heuristic decisions for the integer variables. Nevertheless, in Paper 2 it is shown that the error due to convexifying approximations is small. Moreover, in Paper 5 a method is proposed for improving engine on/off heuristics, which shows that global optimum can be reached for HEVs with a series powertrain topology. However, further studies are needed for improving the gear heuristics.

For problems with one continuous state DP may be the most attractive choice. Some of the reasons are that the problems can be non-convex, nonlinear, mixed-integer; DP problems can be easily parallelized on multiple processors; stochastic information can be easily included, but at the expense

of increasing the size of dynamic states [90]. Furthermore, DP is widely used for HEV powertrain assessment and sizing, with high amount of academic literature and dedicated solvers to speed up computation time [73, 74, 75]. Yet, even for one-state problems, some possibilities that are straightforward in the convex optimization, will significantly decrease the performance of DP. For example, having free final SOC in DP, but still maintaining charge sustain operation, will require running DP iteratively for each gridded SOC as a final state value. Moreover, the constraint on the Ah-throughput of the battery (2.37) will require an additional state in DP.

Perhaps the ultimate solution, as discussed in Paper 5, is a synergy between DP and convex optimization, where DP will be used for optimizing the integer variables and convex optimization for the continuous variables.

5.2 Future studies

It is shown in this thesis that the problem of optimal dimensioning of HEV powertrains can be remodeled to a large extend as a convex problem. The convexifying steps have been performed on both series and parallel powertrains, but still heuristics are needed for the integer variables, such as gear and engine on/off. Hence, improving the heuristics is the major issue that requires further investigations. A promising method is presented in Paper 5 applied to engine on/off control, which shows that the global optimum can be reached by solving a convex problem in several iterations. Further studies are needed for a theoretical foundation to find for which problems the algorithm will converge and for which it may not. Investigations are also needed for extending the strategy to improve gear heuristics.

The convex modeling steps can be extended to other types of hybrid vehicles where the energy storage is e.g. a fuel cell or a flywheel. It is also interesting to investigate is it possible to use convex optimization for HEVs with planetary gears or continuous variable transmission. Future studies may also focus on simultaneous sizing and control of the cooling system for many vehicle components, including the passenger compartment.

The methods developed in this thesis have been applied on several examples that illustrate how the methods work and what are their capabilities. However, to take a reliable decision on designing an HEV the methods need to be applied on more practical examples. For powertrain dimensioning problems in public transportation, there is a need for including realistic and well projected prices for charging stations, fuel, electricity and powertrain components. The short computation time of convex optimization, and the possibility to distribute the optimization on several computers, may allow optimization of charging infrastructure in an entire city and simultaneous

component sizing of several buses driven on several bus lines. For private vehicles, improvements are needed in obtaining well representative driving and charging patterns and a possibility to include performance requirements in the optimization.

References

[1] J. Larminie, J. Lowry, Electric Vehicle Technology Explained, John Wiley & Sons Ltd., 2003.

[2] C. D. Anderson, J. Anderson, Electric and hybrid cars, a history, 2nd Edition, McFarland & Company, Inc., 2010.

[3] D. A. Kirsch, The Electric Vehicle and the Burden of History, Rutgers University Press, 1964.

[4] Jacob Lohner & Co, The first hybrid vehicle, `http://www.hybrid-vehicle.org`, accessed March 2012.

[5] A. Kraytsberg, Y. Ein-Eli, Review on Li-air batteries - Opportunities, limitations and perspective, Journal of Power Sources 196 (3) (2011) 886–893.

[6] J.-G. Zhang, D. Wang, W. Xu, J. Xiao, R. Williford, Ambient operation of Li/Air batteries, Journal of Power Sources 195 (13) (2010) 4332–4337.

[7] L. Gaines, R. Cuenca, Costs of lithium-ion batteries for vehicles, Tech. rep., Center for Transportation Research at Argonne National Labaratory, United States Department of Energy (May 2000).

[8] Honda Motor Corporation, Honda Civic Hybrid and Honda Insight, `http://honda.com`, accessed March 2012.

[9] Volvo Group, Volvo 7900 Hybrid Bus, `http://www.volvo.com`, accessed March 2012.

[10] Daimler Buses North America, Orion VII Hybrid, `http://www.orionbus.com`, accessed March 2012.

[11] Audi AG, Audi A1 e-tron, `http://www.audi.com`, accessed March 2012.

[12] Toyota Motor, Toyota Prius, http://www.toyota.com, accessed March 2012.

[13] M. R. Schmidt, Two-mode, split power, electro-mechanical transmission (November 26 1996).

[14] General Motors, Hybrid & electric vehicles, http://www.gm.com, accessed March 2012.

[15] E. Nordlund, C. Sadarangani, The four-quadrant energy transducer, in: Industry Applications Conference, Pittsburgh, PA, USA, 2002.

[16] AutoTram: Transport system of the future, Tech. rep., Fraunhofer Institute for Transportation and Infrastructure Systems IVI (2010).

[17] R. Bedell, Practical, 70-90% electric bus without overhead wires, in: EVS24, Stavanger, Norway, 2009.

[18] R. Bedell, B. Westerlund, P. Åstrand, First results from field testing of fast charged hybrid buses in Umea, sweden, in: EEVC, Brussels, Belgium, 2011.

[19] M. Johansson, O. Olsson, Feasibility study of dual-mode buses in Gothenburg's public transport, Master's thesis, Chalmers University of Technology, Gothenburg, Sweden (2011).

[20] On-line electric vehicle, Tech. rep., Korea Advanced Institute of Science and Technology (KAIST) (2009).

[21] N. Murgovski, J. Sjöberg, J. Fredriksson, in: A tool for generating optimal control laws for hybrid electric powertrains, 2010.

[22] J. Sowash, A heroic capacity, American Ceramic Society Bulletin 88 (4) (2009) 19–25.

[23] L. Johannesson, Predictive control of hybrid electric vehicles on prescribed routes, Ph.D. thesis, Chalmers University of Technology, Göteborg, Sweden (2009).

[24] T. C. Moore, HEV control strategy: Implications of performance criteria, system configuration and design, and component selection, in: Proceedings of the American Control Conference, Albuquerque, New Mexico, 1997.

[25] L. Triger, J. Paterson, P. Drozdz, Hybrid vehicle engine size optimization, in: SAE Future Transportation Technology Conference and Exposition, San Antonio, Texas, USA, 1993.

[26] M. R. Cuddy, K. B. Wipke, Analysis of the fuel economy benefit of drivetrain hybridization, in: SAE International Congress & Exposition, Detroit, Michigan, 1997.

[27] V. Galdi, L. Ippolito, A. Piccolo, A. Vaccaro, A genetic-based methodology for hybrid electric vehicles sizing, Soft Computing - A Fusion of Foundations, Methodologies and Applications 5 (6) (2001) 451–457.

[28] X. Hu, Z. Wang, L. Liao, Multi-objective optimization of HEV fuel economy and emissions using evolutionary computation, in: SAE World Congress Detroit, Michigan, 2004.

[29] S. M. Lukic, A. Emadi, Effects of drivetrain hybridization on fuel economy and dynamic performance of parallel hybrid electric vehicles, IEEE Transactions on Vehicular Technology 53 (2) (2004) 385–389.

[30] J. M. Miller, P. J. McCleer, M. Everett, E. G. Strangas, Ultracapacitor plus battery energy storage system sizing methodology for HEV power split electronic CVT's, in: IEEE ISIE, Dubrovnik, Croatia, 2005.

[31] C. Holder, J. Gover, Optimizing the hybridization factor for a parallel hybrid electric small car, in: IEEE Vehicle Power and Propulsion Conference, 2006.

[32] D. Rotenberg, A. Vahidi, I. Kolmanovsky, Ultracapacitor assisted powertrains: Modeling, control, sizing, and the impact on fuel economy, in: American Control Conference, Seattle, Washington, USA, 2008.

[33] R. Bellman, Dynamic Programming, Princeton Univ Pr, New Jersey, 1957.

[34] U. Zoelch, D. Schroeder, Dynamic optimization method for design and rating of the components of a hybrid vehicle, International Journal of Vehicle Design 19 (1) (1998) 1–13.

[35] M. Kim, H. Peng, Power management and design optimization of fuel cell/battery hybrid vehicles, Journal of Power Sources 165 (2) (2007) 819–832.

[36] O. Sundström, L. Guzzella, P. Soltic, Torque-assist hybrid electric powertrain sizing: From optimal control towards a sizing law, IEEE Transactions on Control Systems Technology 18 (4) (2010) 837–849.

[37] M. Kim, H. Peng, Combined control/plant optimization of fuel cell hybrid vehicles, in: Proceedings of the 2006 American Control Conference Minneapolis, Minnesota, USA, 2006.

[38] S. J. Moura, D. S. Callaway, H. K. Fathy, J. L. Stein, Tradeoffs between battery energy capacity and stochastic optimal power management in plug-in hybrid electric vehicles, Journal of Power Sources 195 (9) (2010) 2979–2988.

[39] N. Murgovski, J. Sjöberg, J. Fredriksson, A methodology and a tool for evaluating hybrid electric powertrain configurations, Int. J. Electric and Hybrid Vehicles 3 (3) (2011) 219–245.

[40] T. Hofman, M. Steinbuch, R. van Druten, A. Serrarens, Parametric modeling of components for selection and specification of hybrid vehicle drivetrains, WEVA Journal 1 (1) (2007) 215–224.

[41] T. Hofman, M. Steinbuch, R. van Druten, A. Serrarens, Hybrid component specification optimisation for a medium-duty hybrid electric truck, Int. J. Heavy Vehicle Systems 15 (2/3/4) (2008) 256–392.

[42] E. D. Tate, S. P. Boyd, Finding ultimate limits of performance for hybrid electric vehicles, in: SAE Technical Paper 2000-01-3099, 2000.

[43] R. Trigui, B. Jeanneret, F. Badin, System modelling of hybrid vehicles in order to predict their energy and dynamic performance: Building VEHLIB library, Recherche Transports Sécurité 83 (2) (2004) 129–150.

[44] J. Bumby, P. Clarke, I. Forster, Computer modelling of the automotive energy requirements for internal combustion engine and battery electric-powered vehicles, IEE proceedings 132 (5).

[45] G. H. Cole, SIMPLEV: A simple electric vehicle simulation program version 1.0, EG and G Idaho, Inc., Idaho Falls, United States, 1991.

[46] K. Wipke, M. Cuddy, S. Burch, ADVISOR 2.1: A user-friendly advanced powertrain simulation using a combined backward/forward approach, IEEE Transactions on Vehicular Technology.

[47] T. Markel, A. Brooker, T. Hendricks, V. Johnson, K. Kelly, B. Kramer, M. O'Keefe, S. Sprik, K. Wipke, ADVISOR: a systems analysis tool for advanced vehicle modeling, Journal of Power Sources 110 (2) (2002) 255–266.

[48] L. Guzzella, A. Amstutz, CAE tools for quasi-static modeling and optimization of hybrid powertrains, IEEE Transactions on Vehicular Technology 48 (6).

[49] F. D. Torrisi, A. Bemporad, HYSDEL-a tool for generating computational hybrid models for analysis and synthesis problems, IEEE transactions on control systems technology 12 (2).

[50] J. Fredriksson, J. Larsson, J. Sjöberg, P. Krus, Evaluating hybrid electric and fuel cell vehicles using the CAPSim simulation environment, in: Proceedings of the 22nd International Battery Hybrid and Fuel Cell Electric Vehicle Symposium and Exposition, Yokohama, Japan, 2006.

[51] K. L. Butler, M. Ehsani, P. Kamath, A Matlab-based modeling and simulation package for electric and hybrid electric vehicle design, IEEE Transactions on Vehicular Technology 48 (6).

[52] J. V. Mierlo, G. Maggetto, Vehicle simulation program: a tool to evaluate hybrid power management strategies based on an innovative iteration algorithm, Proc Instn Mech Engrs 215 Part D.

[53] O. Hayat, M. Lebrun, E. Domingues, Powertrain drivability evaluation: Analysis and simplification of dynamic models, in: SAE World Congress, Detroit, Michigan, 2003.

[54] J. Liu, H. Peng, Automated modelling of power-split hybrid vehicles, in: Proceedings of the 17th World Congress The International Federation of Automatic Control, Seoul, Korea, 2008.

[55] J. Kang, I. Kolmanovsky, J. Grizzle, Approximate dynamic programming solutions for lean burn engine aftertreatment, in: Proceedings of the 38th IEEE Conference on Decision and Control, Vol. 2, 1999, pp. 1703–1708.

[56] I. V. Kolmanovsky, S. N. Sivashankar, J. Sun, Optimal control-based powertrain feasibility assessment: A software implementation perspective, in: American Control Conference, Portland, OR, USA, 2005.

[57] C. Lin, H. Peng, J. W. Grizzle, J. Kang, Power management strategy for a parallel hybrid electric truck, IEEE transactions on control systems technology 11 (6).

[58] O. Sundström, L. Guzzella, P. Soltic, Optimal hybridization in two parallel hybrid electric vehicles using Dynamic Programming, in: Proceedings of the 17th World Congress The International Federation of Automatic Control, Seoul, Korea, 2008.

[59] G. Rizzoni, L. Guzzella, B. M. Baumann, Unified modeling of hybrid electric vehicle drivetrains, IEEE/ASME Trans. Mechatron. 4 (3) (1999) 246–257.

[60] X. Wei, G. Rizzoni, A scalable approach for energy converter modeling and supervisory control design, Proc. ASME Int. Mech. Eng. Congr. Expos. (2001) 1281–1288.

[61] S. Boyd, L. Vandenberghe, Convex Optimization, Cambridge University Press, 2004.

[62] H. Witsenhausen, A class of hybrid-state continuous-time dynamic systems, IEEE Transactions on Automatic Control 11 (2) (1996) 161–167.

[63] P. Pisu, G. Rizzoni, A comparative study of supervisory control strategies for hybrid electric vehicles, IEEE Transactions on Control Systems Technology 15 (3) (2007) 506–518.

[64] A. Sciarretta, L. Guzzella, Control of hybrid electric vehicles, IEEE Control Systems Magazine 27 (2) (2007) 60–70.

[65] D. Ambühl, O. Sundström, A. Sciarretta, L. Guzzella, Explicit optimal control policy and its practical application for hybrid electric powertrains, Control Engineering Practice 18 (12) (2010) 1429–1439.

[66] S. J. Pachernegg, A closer look at the willans-line, SAE Technical Paper, 1969, doi:10.4271/690182.

[67] L. Guzzella, C. H. Onder, Introduction to Modeling and Control of Internal Combustion Engine Systems, Springer-Verlag, 2010.

[68] M. Neuman, H. Sandberg, B. Wahlberg, A. Folkesson, Modelling and control of series HEVs including resistive losses and varying engine efficiency, in: SAE International, 2008.

[69] A. F. Burke, Batteries and ultracapacitors for electric, hybrid, and fuel cell vehicles, Proceedings of the IEEE 95 (4) (2007) 806–820.

[70] A. F. Burke, Ultracapacitors: why, how, and where is the technology, Journal of Power Sources 91 (2000) 37–50.

[71] O. Sundström, Optimal control and design of hybrid-electric vehicles, Ph.D. thesis, Institute for Dynamic Systems and Control, ETH Zurich (2009).

[72] M. Pourabdollah, N. Murgovski, A. Grauers, B. Egardt, Optimal sizing of a parallel PHEV powertrain, IEEE Transactions on Vehicular Technology.

[73] O. Sundström, L. Guzzella, A generic Dynamic Programming Matlab function, in: 18th IEEE International Conference on Control Applications, Saint Petersburg, Russia, 2009.

[74] O. Sundström, D. Ambühl, L. Guzzella, On implementation of Dynamic Programming for optimal control problems with final state constraints, Oil Gas Sci. Technol. 65 (1) (2009) 91–102.

[75] P. Elbert, S. Ebbesen, L. Guzzella, Implementation of Dynamic Programming for n-dimensional optimal control problems with final state constraints, IEEE Transactions on Control Systems Technology (2012).

[76] Y. Labit, D. Peaucelle, D. Henrion, SeDuMi interface 1.02: a tool for solving LMI problems with SeDuMi, IEEE International Symposium on Computer Aided Control System Design Proceedings (2002) 272–277.

[77] K. C. Toh, R. H. Tütüncü, M. J. Todd, On the implementation and usage of SDPT3 - a Matlab software package for semidefinite-quadratic-linear programming, version 4.0 (July 2006).

[78] W. R. Hamilton, On a general method in dynamics, Philosophical Transactions of the Royal Society 2 (1834) 247–308.

[79] W. R. Hamilton, Second essay on a general method in dynamics, Philosophical Transactions of the Royal Society 1 (1835) 95–144.

[80] G. A. Bliss, The problem of Lagrange in the calculus of variations, American Journal of Mathematics 52 (4) (1930) 673–744.

[81] E. J. McShane, On multipliers for Lagrange problems, American Journal of Mathematics 61 (4) (1939) 809–819.

[82] L. S. Pontryagin, V. G. Boltyanskii, R. V. Gamkrelidze, E. F. Mishchenko, The mathematical theory of optimal processes, Interscience publishers, 1962.

[83] L. Guzzella, A. Sciarretta, Vehicle propulsion systems, introduction to modeling and optimization, 2nd Edition, Springer, Berlin, Heidelberg, 2007.

[84] T. Hofman, Framework for combined control and design optimization of hybrid vehicle propulsion systems, Ph.D. thesis, Eindhoven University of Technology (2007).

[85] S. Delprat, J. Lauber, T. M. Guerra, J. Rimaux, Control of a parallel hybrid powertrain: optimal control, IEEE Transactions on Vehicular Technology 53 (3) (2004) 872–881.

[86] X. Wei, L. Guzzella, V. I. Utkin, G. Rizzoni, Model-based fuel optimal control of hybrid electric vehicle using variable structure control systems, Journal of Dynamic Systems, Measurement, and Control 129 (1) (2007) 13–19.

[87] M. Grant, S. Boyd, CVX: Matlab software for disciplined convex programming, version 1.21, `http://cvxr.com/cvx` (May 2010).

[88] J. Löfberg, YALMIP: A toolbox for modeling and optimization in Matlab, In Proceedings of the CACSD Conference, Taipei, Taiwan, `http://users.isy.liu.se/johanl/yalmip` (2004).

[89] S. Boyd, N. Parikh, E. Chu, Distributed Optimization and Statistical Learning via the Alternating Direction Method of Multipliers, Now Publishers Inc, 2011.

[90] L. Johannesson, M. Åsbogård, B. Egardt, Assessing the potential of predictive control for hybrid vehicle powertrains using stochastic Dynamic Programming, IEEE Transactions on Intelligent Transportation Systems 8 (1) (2007) 71–83.